Phys. Lett. B 854 (2024) 138743

Contents lists available at ScienceDirect

Physics Letters B

journal homepage: www.elsevier.com/locate/physletb

Letter

Search for pair-production of vector-like quarks in lepton+jets final states containing at least one b-tagged jet using the Run 2 data from the ATLAS experiment

The ATLAS Collaboration *

ARTICLE INFO

Editor: M. Doser

ABSTRACT

A search is presented for the pair-production of heavy vector-like quarks in the lepton+jets final state using 140 fb^{-1} of proton–proton collisions at $\sqrt{s} = 13$ TeV collected with the ATLAS detector. The search is optimised for vector-like top-quarks (T) that decay into a W boson and a b-quark, with one W boson decaying leptonically and the other hadronically. Other vector-like quark flavours and decay modes are also considered. Events are selected with one high transverse-momentum electron or muon, large missing transverse momentum, a large-radius jet identified as a W boson, and multiple small-radius jets, at least one of which is b-tagged. Vector-like T-quarks with 100% branching ratio to Wb are excluded at 95% CL for masses below 1700 GeV. These limits are also applied to vector-like Y-quarks, which decay exclusively into a W boson and a b-quark. Isospin singlets with $\mathcal{B}(T \to Wb : Ht : Zt) = 1/2 : 1/4 : 1/4$ are excluded for masses below 1360 GeV.

1. Introduction

The Standard Model (SM) of particle physics is extremely successful in describing elementary particles and their interactions, yet its many shortcomings reveal that it is incomplete. In particular, naturalness [1] suggests that a more complete theory will provide an explanation for how radiative divergences to the Higgs boson mass from t-quark loops are cancelled out. Extensions of the SM, such as extra dimensions [2], composite Higgs bosons [3,4] and Little Higgs boson [5] models, predict the existence of vector-like quarks (VLQs) that could mitigate these large radiative corrections to the Higgs boson mass. The VLQs are spin-1/2, colour-triplets that have the same weak isospin for left- and right-handed chiralities. Thus, VLQs would not acquire mass via the Higgs boson [6], allowing them to evade the limits that exclude additional SM-like quarks [7]. To cancel out the Higgs boson mass divergence from top-quark loops, the VLQs must couple preferentially to third-generation quarks. VLQs could appear as different types of multiplets: SU(2) singlets, doublets, or triplets of T, B, X or Y; where T and B have the same electric charge as the SM t- and b-quarks, while X and Y have electric charges 5/3 and −4/3, respectively. In the simplest models, the mass difference between VLQs in a given SU(2) multiplet must be small to satisfy constraints from precision electroweak measurements [6], excluding cascade decays such as $T \to WB \to WWt$. The VLQs can decay via a flavour-changing neutral current or a charged current, allowing the T and B to each have three possible decays: $T \to Wb/Zt/Ht$ and $B \to Wt/Zb/Hb$. The X and Y have no SM partners, so these can only decay via $X \to Wt$ and $Y \to Wb$. Decays into final states with first and second generation quarks, though not forbidden, are not favoured as they would not address the hierarchy problem. Examples of Feynman diagrams for T and B pair production and decay are shown in Fig. 1.

The branching ratio of the VLQ decay to SM particles is not fixed by the theory, therefore, all possible VLQ decays and branching ratios need to be probed in searches for VLQs. A combination of searches for pair-production of VLQs by ATLAS using 36 fb^{-1} of Run 2 data collected at the Large Hadron Collider (LHC) from 2015 to 2016 at a centre-of-mass energy of $\sqrt{s} = 13$ TeV excludes VLQs with masses below 1310 GeV for any branching ratio to the assumed decays [8]. ATLAS searches for pair-produced VLQs using the full proton–proton (pp) collision data sample of 140 fb^{-1} collected during Run 2 of the LHC between 2015 and 2018 at $\sqrt{s} = 13$ TeV include a search in final states with one lepton, jets and large missing transverse momentum [9], mostly sensitive to the decay $T \to Zt$ or $B \to Wt$, and in final states with at least one leptonically decaying Z boson and a third-generation quark [10], which is mainly sensitive to $T \to Zt$ and $B \to Zb$. CMS published searches for pair production [11,12] of vector-like quarks using 137 fb^{-1} of data collected during the LHC Run 2.

ATLAS has previously performed a search for pair-produced VLQs in the one lepton+jets final state using 36 fb^{-1} of Run 2 data which was optimised to the $T \to Wb$ decay [13]. That search excluded T-

* E-mail address: atlas.publications@cern.ch.

https://doi.org/10.1016/j.physletb.2024.138743
Received 31 January 2024; Received in revised form 15 May 2024; Accepted 20 May 2024
Available online 23 May 2024

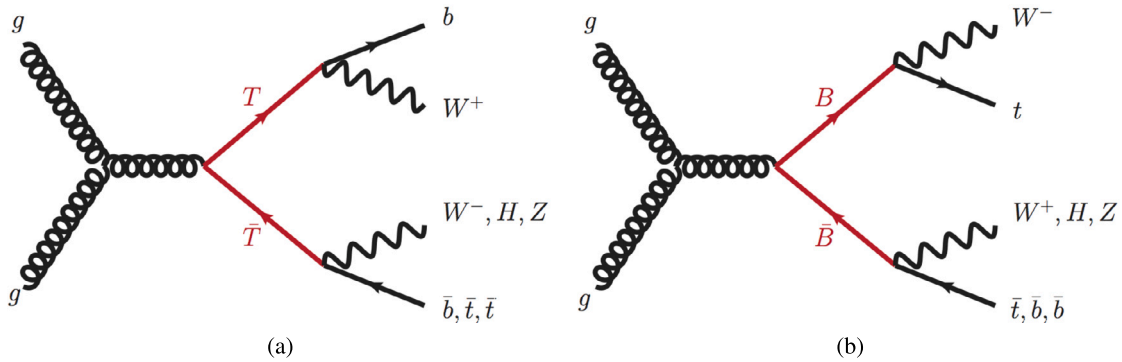

Fig. 1. Representative tree-level Feynman diagrams for (a) $T\bar{T}$ and (b) $B\bar{B}$ production for which at least one of the VLQs decays into a W boson.

quark masses below 1350 GeV in the scenario $\mathcal{B}(T \to Wb) = 1$ and T-quark masses below 1170 GeV in the T isospin singlet scenario with a branching ratio of $\mathcal{B}(T \to Wb : Ht : Zt) = 1/2 : 1/4 : 1/4$. The recent search for pair-produced VLQs by CMS in leptonic final states using the full CMS Run 2 data sample excludes the scenario $\mathcal{B}(T \to Wb) = 1$ for masses below 1540 GeV [12].

Singly produced VLQs have also been searched for by ATLAS [14,15] and CMS [16–18] using the full LHC Run 2 data sample, but the interpretation of the search results depends on an additional constant for the coupling to electroweak bosons [19].

This paper presents a search for the pair production of VLQs decaying into third-generation quarks using the pp collision data collected at the LHC from 2015 to 2018 at a centre-of-mass energy of 13 TeV with the ATLAS experiment, increasing the data sample relative to the previous search in this decay channel from 36 fb^{-1} to 140 fb^{-1}. The analysis is optimised for the $T\bar{T} \to WbW\bar{b}$ channel with one W boson decaying leptonically and the other hadronically, resulting in a final state with exactly one lepton, missing transverse momentum and jets, but the search is also sensitive to the other VLQs and decay modes. Targeting events with a leptonically decaying W boson ($W \to \ell\nu$ with $\ell = e, \mu$) suppresses SM processes with purely hadronic final states, while the hadronically decaying W boson provides a large branching ratio. Vector-like T candidates are reconstructed such that the mass difference between the leptonically and hadronically decaying T candidates is minimised. The reconstructed mass of the leptonically decaying T is then used as the discriminating variable to test for the presence of a VLQ signal. The dominant background processes are $t\bar{t}$, W+jets, and single-top-quark production. Control regions enhanced in $t\bar{t}$ or W+jets events are used to correct the mismodelling observed in Monte-Carlo (MC) simulations of those processes. Finally, a profile likelihood fit is performed on the observed distributions of the reconstructed VLQ mass to test for the presence of VLQ signals for various signal models, varying the VLQ mass and the decay branching ratios. The data-driven corrections to $t\bar{t}$ and W+jets in dedicated control regions are new with respect to previous analyses. The statistical analysis also includes additional control regions to better constrain the dominant backgrounds characterised by substantial modelling uncertainties, while maintaining a high signal acceptance and achieving a narrow peak in the reconstructed VLQ mass distribution. Further improvements are brought by the improved object identification, especially from W-boson tagging.

2. ATLAS detector

The ATLAS experiment [20] at the LHC is a multipurpose particle detector with a forward–backward symmetric cylindrical geometry and a near 4π coverage in solid angle.[1] It consists of an inner tracking detector (ID) surrounded by a thin superconducting solenoid providing a 2 T axial magnetic field, electromagnetic and hadron calorimeters, and a muon spectrometer. The inner tracking detector covers the pseudorapidity range $|\eta| < 2.5$. It consists of silicon pixel, silicon microstrip, and transition radiation tracking detectors. Lead/liquid-argon (LAr) sampling calorimeters provide electromagnetic (EM) energy measurements with high granularity. A steel/scintillator-tile hadron calorimeter covers the central pseudorapidity range ($|\eta| < 1.7$). The endcap and forward regions are instrumented with LAr calorimeters for both the EM and hadronic energy measurements up to $|\eta| = 4.9$. The muon spectrometer (MS) surrounds the calorimeters and is based on three large superconducting air-core toroidal magnets with eight coils each. The field integral of the toroids ranges between 2.0 and 6.0 T m across most of the detector. The muon spectrometer includes a system of precision tracking chambers and fast detectors for triggering. A two-level trigger system is used to select events. The first-level trigger is implemented in hardware and uses a subset of the detector information to accept events at a rate below 100 kHz. This is followed by a software-based trigger that reduces the accepted event rate to 1 kHz on average depending on the data-taking conditions. An extensive software suite [21] is used in data simulation, in the reconstruction and analysis of real and simulated data, in detector operations, and in the trigger and data acquisition systems of the experiment.

3. Data and simulated event samples

The data sample analysed is from pp collisions with a centre-of-mass energy of $\sqrt{s} = 13$ TeV. The data were collected between 2015 and 2018 with the ATLAS detector and correspond to an integrated luminosity of 140 fb^{-1} [22,23]. A set of single-electron [24] and single-muon triggers [25] were used, with transverse momentum (p_{T}) lowest thresholds in the range of 20–26 GeV depending on the lepton flavour and data-taking period. In addition, data were recorded using a trigger targeting events with large missing transverse energy ($E_{\mathrm{T}}^{\mathrm{miss}}$) [26] with thresholds of 70, 90 or 110 GeV, depending on the data taking period. All detector subsystems are required to be operational during data taking and to satisfy data quality requirements [27].

Signal events and SM background with at least one prompt lepton are modelled by MC simulation. Contributions from processes surviving selection requirements due to non-prompt leptons or hadronic jets misidentified as leptons (dominated by QCD multijet events) are estimated by a data-driven method, with MC samples serving as cross checks. All samples were produced using the ATLAS simulation infrastructure [28] and GEANT4 [29]. The estimate of some systematic

[1] ATLAS uses a right-handed coordinate system with its origin at the nominal interaction point (IP) in the centre of the detector and the z-axis along the beam pipe. The x-axis points from the IP to the centre of the LHC ring, and the y-axis points upwards. Polar coordinates (r, ϕ) are used in the transverse plane, ϕ being the azimuthal angle around the z-axis. The pseudorapidity is defined in terms of the polar angle θ as $\eta = -\ln\tan(\theta/2)$. Angular distance is measured in units of $\Delta R \equiv \sqrt{(\Delta\eta)^2 + (\Delta\phi)^2}$.

uncertainties used a faster detector simulation employing a parameterisation of the calorimeter response [30]. Unless specified otherwise, the parton shower, hadronisation, and underlying events are modelled using PYTHIA8.230 [31], with parameters set according to the A14 set of tunable parameters (the A14 "tune") [32] and using the NNPDF2.3LO set of parton distribution functions (PDFs) [33]. In the simulation, the t-quark and SM Higgs boson masses were set to 172.5 GeV and 125 GeV, respectively. The effect of additional pp interactions per bunch crossing (pile-up) is accounted for by overlaying the hard-scattering process with minimum-bias events simulated with PYTHIA 8.186 [34] using the A3 tune [35] and NNPDF2.3LO PDFs. The distribution of the mean number of interactions per bunch crossing in simulation is reweighted such that its distribution matches that measured in the data.

Signal events for the production and decay of $T\bar{T}$ and $B\bar{B}$ were simulated at leading-order using PROTOS v.2.2 [36] with VLQ masses from 1000 GeV to 1800 GeV in steps of 100 GeV, and with a mass of 2000 GeV. The samples were produced for the singlet model, with alternative branching ratio scenarios obtained by reweighting the events based on the decay mode. Samples for the doublet model with a mass of 1.2 TeV were also produced to confirm that kinematic differences due to isospin have negligible impact on the results. The signal cross-sections were calculated with TOP++ 2.0 [37] at next-to-next-to-leading-order (NNLO) in QCD including the resummation of next-to-next-to-leading-logarithmic (NNLL) soft-gluon terms.

The dominant background arises from the production of t-quark pairs ($t\bar{t}$). Events with a single t-quark (henceforth referred to as "single top") or a W boson produced in association with jets (W+jets) also make significant contributions. Finally, events containing a Z boson and jets (Z+jets), three or four t-quarks, multi-boson events, and t-quark pairs produced in association with a vector boson or a Higgs boson (ttV with $V = W, Z$ and ttH, respectively) have small contributions.

The production of $t\bar{t}$ events is modelled using the POWHEG BOX v2 [38–41] generator at NLO accuracy in QCD with the NNPDF3.0NLO [42] PDFs and the h_{damp} parameter[2] set to $1.5m_t$ [43], where m_t denotes the t-quark mass. The dependence on the parton shower and hadronisation models is evaluated by comparing the nominal $t\bar{t}$ sample with an alternative sample also produced with POWHEG BOX v2 generator using the NNPDF3.0NLO PDFs, but instead interfaced to HERWIG7.04 [44,45] using the MMHT2014LO PDFs [46] and the H7UE tune [45]. An uncertainty in the matching of the NLO matrix elements (ME) to the parton shower is assessed by comparing the nominal sample to one simulated with MADGRAPH5_AMC@NLO 2.6.0 [47] using the NNPDF3.0NLO PDFs. The effect from possibly under-estimating the initial-state radiation (ISR) is evaluated by comparing the nominal sample to one produced with h_{damp} increased to $3m_t$, the renormalisation and factorisation scales divided by two, and using the "Var3cUp" weight of the A14 tune. The effect from possibly over-estimating the ISR is evaluated by comparing the nominal sample to one obtained by doubling the renormalisation and factorisation scales and choosing the "Var3cDown" weight of the A14 tune [48]. The size of the uncertainty in the modelling of final state radiation (FSR) is evaluated by doubling or halving the renormalisation scale for emissions from the parton shower.

The associated production of a t-quark with a W boson (tW) accounts for the vast majority of single top events. These events were modelled with the POWHEG BOX v2 generator at NLO in QCD using the five-flavour scheme and the NNPDF3.0NLO PDFs. The nominal sample uses the diagram removal (DR) scheme [49] to remove the contribution from Feynman diagrams already included in the $t\bar{t}$ production. An alternative sample simulated using the diagram subtraction scheme (DS) [43,49] is used to evaluate an uncertainty due to the choice of $t\bar{t}/tW$ overlap removal scheme. The uncertainty due to the parton shower and hadronisation models is evaluated by comparing the nominal sample of events with events simulated by the POWHEG BOX v2 generator interfaced to HERWIG7.04 using the H7UE tune and the MMHT2014LO PDFs. To assess the uncertainty in the matching of the ME to the parton shower, the nominal tW sample is compared with a sample simulated with the MADGRAPH5_AMC@NLO 2.6.2 generator at NLO in QCD using the five-flavour scheme and the NNPDF2.3LO PDFs [42].

The small contributions from single top t-channel and s-channel production were modelled using the POWHEG BOX v2 [39–41,50,51] generator at NLO in QCD using the four-flavour scheme (t-channel) or the five-flavour scheme (s-channel) and the NNPDF3.0NLO PDFs. The uncertainty due to the parton shower and hadronisation models is evaluated by comparing the nominal sample of events with events simulated by the POWHEG BOX v2 generator at NLO accuracy in QCD using the five-flavour scheme and interfaced to HERWIG7.04 using the H7UE tune and the MMHT2014LO PDFs. To assess the uncertainty in the matching of NLO accuracy ME to the parton shower, the nominal sample is compared with a sample simulated with the MADGRAPH5_AMC@NLO 2.6.2 generator at NLO accuracy in QCD using the five-flavour scheme and NNPDF2.3NLO or NNPDF3.0NLO PDFs for the t- and s-channel, respectively.

The production of V+jets ($V = W, Z$) was simulated with the SHERPA2.2.1 [52] generator at NLO accuracy in QCD for up to two partons, and at LO accuracy for up to four additional partons. The full samples are then normalised to the NNLO predictions [53]. Samples of diboson events (VV) were simulated with the SHERPA2.2.1 or 2.2.2 [52] generator at NLO accuracy in QCD for up to one additional parton and at LO accuracy for up to three additional parton emissions, including off-shell effects and Higgs-boson contributions, where appropriate. The ME calculations for SHERPA samples were matched and merged with the parton shower based on Catani–Seymour dipole factorisation [54,55] using the MEPS@NLO prescription. The virtual QCD corrections were provided by the OPENLOOPS library [56–58]. The NNPDF3.0NNLO set of PDFs was used, along with the dedicated tune developed by the SHERPA authors.

The production of $t\bar{t}V$ and tWZ events was modelled using the MADGRAPH5_AMC@NLO 2.3.3 generator at NLO with the NNPDF3.0NLO PDF and PYTHIA8.210 (PYTHIA8.211) for $t\bar{t}V$ (tWZ) with the A14 tune and the NNPDF2.3LO PDFs for the parton shower and hadronisation. The diagram removal scheme described in Ref. [49] was employed to treat the overlap between tWZ and $t\bar{t}Z$, and was applied to the tWZ sample. The production of $t\bar{t}H$ events is modelled using the POWHEG BOX v2 generator at NLO with the NNPDF3.0NLO PDF set. The production of tZ, three and four t-quarks events, and $t\bar{t}WW$ events was simulated with MADGRAPH5_AMC@NLO 2.2.2 interfaced to PYTHIA8.186 using the A14 tune. The small contributions from processes from $t\bar{t}H$, tWZ, tZ, $ttWW$ and multi-top production are summarised as "rare top" processes. Multijet MC samples were simulated using the SHERPA 2.1.1 generator. The matrix element calculation was included for the $2 \to 2$ process at leading-order, and the default SHERPA parton shower based on Catani–Seymour dipole factorisation was used for the showering with p_{T} ordering, using the CT10 PDF set [59].

Decays of b- and c-hadrons were simulated by EVTGEN 1.6.0 [60] in all simulations except SHERPA, for which the default SHERPA configuration recommended by the SHERPA authors was used.

4. Object reconstruction

Events are required to contain at least one vertex with two or more associated tracks that must have $p_T > 500$ MeV. Among all vertices, the vertex with the highest p_T^2 sum of the associated tracks is taken as the primary vertex (PV) [61].

[2] The h_{damp} parameter is a resummation damping factor and one of the parameters that controls the matching of POWHEG matrix elements (ME) to the parton shower and thus effectively regulates the high-p_{T} radiation against which the $t\bar{t}$ system recoils.

Electrons are reconstructed from clusters in the EM calorimeter matched with ID tracks and are calibrated [62]. Electron candidates must be in the central region of the detector ($\left|\eta\right| < 2.47$) with $p_{\mathrm{T}} > 27$ GeV and match a track with $\left|z_0 \sin\theta\right| < 0.5$ mm and $\left|d_0/\sigma_{d_0}\right| < 5$; where d_0 is the impact parameter between the track and the beam line, σ_{d_0} is the measured uncertainty in d_0, and z_0 is the minimum distance in z between the track and the beam spot. Any candidates in the transition region between the barrel and endcap calorimeters ($1.37 < |\eta| < 1.52$) are removed. "Baseline electrons" must satisfy the *medium likelihood* identification criteria [62], with no selection on the isolation. "Tight electrons" must satisfy the *tight likelihood* identification criteria, plus the following isolation requirements in both the calorimeter and the ID [62]. The first isolation requirement is $E^{\mathrm{isol}}_{\mathrm{T,\,cone}}/p^{e}_{\mathrm{T}} < 0.2$; where p^{e}_{T} is the electron candidate p_{T} and $E^{\mathrm{isol}}_{\mathrm{T,cone}}$ is the energy deposited in the calorimeter within a cone of size $R = 0.2$ around the candidate direction; any leakage energy and energy from pile-up are subtracted. The second isolation requirement is $p^{\mathrm{isol}}_{\mathrm{T,var}}/p^{e}_{\mathrm{T}} < 0.15$; where $p^{\mathrm{isol}}_{\mathrm{T,var}}$ is the sum of the track p_{T} without the electron candidate in a cone of radius $R = \min(10\,\mathrm{GeV}/p^{e}_{\mathrm{T}}, 0.2)$. Scale factors are used to correct for differences between data and simulation for reconstruction, identification, isolation and trigger selection efficiencies [62].

Muons are reconstructed [63] from combined tracks in the MS and the ID, with "baseline muons" required to satisfy the *loose* identification criteria and no selection on the isolation, while "tight muons" must satisfy the *tight* identification criteria [63] and satisfy the track-based isolation requirements defined by the *TightTrackOnly* working point. This working point uses the scalar sum of the p_{T} of all tracks that are within a cone of size $R = \min(0.3, 10\,\mathrm{GeV}/p^{\mu}_{\mathrm{T}})$ around the muon candidate, where p^{μ}_{T} is the candidate muon p_{T}. The track matched to the muon candidate under consideration is excluded from the sum. The muon is selected if this sum is less than 6% of p^{μ}_{T}. Finally, all muon candidates are required to satisfy $|z_0 \sin\theta| < 0.5$ mm and $\left|d_0/\sigma_{d_0}\right| < 3$. Muons are calibrated [64] and are required to have $p_{\mathrm{T}} > 15$ GeV and to be reconstructed within $|\eta| = 2.5$. Scale factors are used to correct for differences in muon reconstruction, identification, vertex matching, isolation and trigger efficiencies between simulation and data [63].

Small-radius (small-R) jet candidates are built from particle-flow objects [65], using the anti-k_t algorithm [66,67] with a radius parameter of $R = 0.4$. The particle-flow algorithm combines information about tracks in the ID and energy deposits in the calorimeters to form the input for the jet reconstruction. The jet energy is calibrated to the particle level scale by using a sequence of corrections, including simulation-based corrections and in situ calibrations [68]. Jets are required to have $p_{\mathrm{T}} > 25$ GeV and $|\eta| < 2.5$. To reject jets originating from pile-up interactions, jet candidates with $|\eta| < 2.4$ and $p_{\mathrm{T}} < 60$ GeV are required to satisfy the "tight" jet vertex tagger (JVT) criterion [69]. An algorithm based on deep and recurrent neural networks, called DL1r, is used to identify small-R jets containing a b-hadron decay [70]. Jets are considered to be b-tagged if they satisfy the criteria for the operating point with an efficiency of 77% and mistag rates for charm and light jets of 17.7% and 0.52%, respectively, as determined in simulated $t\bar{t}$ events. The b-quark tagging efficiencies in simulation, and the charm and light jet mistag rates, are corrected to match the efficiencies in data [71–73].

An overlap removal procedure is applied to prevent double counting of ambiguous reconstructed objects, using the baseline lepton definitions. First, electron–muon overlap is handled by removing muons sharing a track in the ID with an electron if the muon is calorimeter-tagged [63], and otherwise removing the electron. Next, overlap between jets and leptons is removed by rejecting any jets within $\Delta R = 0.2$ of an electron, followed by the rejection of any electrons within $\Delta R = 0.4$ of the remaining jets. Similarly, jets are discarded if they have fewer than three matched tracks and are within $\Delta R = 0.2$ of a muon candidate. Otherwise, the muon is rejected if it lies within $\Delta R = \min(0.4, 0.04 + 10\,\mathrm{GeV}/p^{\mu}_{\mathrm{T}})$ of a jet.

The missing transverse momentum, with magnitude $E^{\mathrm{miss}}_{\mathrm{T}}$, is defined as the negative vectorial sum of the transverse momenta of all calibrated objects in an event, plus a track-based soft-term which takes into account energy depositions matched to the primary vertex but not matched with any calibrated object [74].

Finally, large-radius (large-R) jets are constructed from the noise-suppressed topological calorimeter-cell clusters calibrated by using local hadronic cell reweighting [75] and the anti-k_t algorithm with $R = 1.0$. To reduce the impact of soft radiation, a grooming algorithm called "trimming" [76] is applied. Constituent small-R jets, reclustered with the k_t algorithm with a radius parameter $R = 0.2$, with p_{T} less than 5 % of the large-R jet p_{T} are removed. The large-R jets are required to have $p_{\mathrm{T}} > 200$ GeV, $|\eta| < 2.0$ and a mass larger than 50 GeV. The jet energy scale (JES) and resolution (JER) and the mass scale (JMS) and resolution (JMR) of large-radius jets are calibrated [77,78]. A W boson tagging algorithm identifies high-p_{T} hadronically decaying W bosons, whose decay products are collimated to a single large-radius jet [79], with an efficiency of 80%. The W-tagging algorithm applies criteria on the mass of the large-radius jet, the number of inner-detector tracks associated with the jets and the energy correlation function ratio D_2 [79,80]. Scale factors correct the W boson tagging efficiency in simulation to match the efficiency measured in data [81].

5. Event selection, reconstruction and categorisation

This search targets final states with exactly one electron or muon, missing transverse momentum, and jets. Events are selected by a single lepton or $E^{\mathrm{miss}}_{\mathrm{T}}$ trigger, as described in Section 3. If the event is selected by a single lepton trigger, the selected lepton must have $p_{\mathrm{T}} > 27$ GeV and be matched to the object that triggered the event. If the event is selected by the $E^{\mathrm{miss}}_{\mathrm{T}}$ trigger, it must have $E^{\mathrm{miss}}_{\mathrm{T}} > 200$ GeV. The $E^{\mathrm{miss}}_{\mathrm{T}}$ trigger selection is added to compensate for the efficiency loss of the single muon triggers at high muon p_{T}. These lepton and the $E^{\mathrm{miss}}_{\mathrm{T}}$ requirements ensure full trigger efficiency over all data taking periods.

Events are required to have exactly one tight muon with $p_{\mathrm{T}} > 27$ GeV or one tight electron with $p_{\mathrm{T}} > 60$ GeV. Increasing the p_{T} threshold for electrons to $p_{\mathrm{T}} > 60$ GeV facilitates the estimation of the background from non-prompt electrons. The fake lepton background estimation relies on the fact that, compared to real leptons, fake leptons that satisfy the baseline lepton selection have a much lower efficiency for satisfying the tight lepton criteria. The single electron trigger selection, which is part of both the baseline and tight electron selection already imposes very strict selections on the electrons with $p_{\mathrm{T}} < 60$ GeV, making it difficult to define a selection tighter than the baseline electron criteria. Studies showed that increasing the electron p_{T} threshold to 60 GeV does not impact the analysis sensitivity. Events with additional leptons with $p_{\mathrm{T}} > 25$ GeV satisfying the baseline criteria are vetoed. In addition, all events must have $E^{\mathrm{miss}}_{\mathrm{T}} > 60$ GeV and contain at least three small-R jets, at least one of which must be b-tagged. The criteria described above are referred to as the preselection.

The focus is on T-quarks with a mass above 1.35 TeV, which corresponds to the lower mass limit set by the previous analysis [13]. The large mass of the T will lead to decay products with large p_{T}, which in turn will have collimated decay products. In particular, the hadronically decaying W boson will produce a large-R jet, so events are required to contain at least one W-tagged large-R jet. If more than one large-R jet is W-tagged, the one with a mass closest to the W-boson mass ($m_W = 80.38$ GeV) is selected as the hadronically decaying W boson (W_{had}) for the reconstruction of the hadronically decaying T-quark candidate. The leptonically decaying W boson (W_{lep}) is reconstructed from the system of the selected lepton and reconstructed neutrino. The $\vec{p}_T$ of the reconstructed neutrino is determined from the missing transverse momentum, and the p_z of the reconstructed neutrino is calculated by assuming that the lepton-neutrino system has the invariant mass of the W boson. This leads to a quadratic equation. When two real solutions are obtained, the one with the smaller absolute value for the

reconstructed neutrino p_z is used. When the solutions are complex, a real solution is obtained by adjusting the x and y components of the neutrino momentum to minimise a χ^2 parameter that includes the uncertainties in the neutrino and lepton momenta and W boson mass. Finally, the angular distance between the lepton and the reconstructed neutrino is required to be $\Delta R(\ell, \nu) < 0.7$.

Reconstruction of the two T candidates is done by pairing each of the W candidates, W_{lep} and W_{had}, with a small-R jet. The small-R jets are selected for pairing with the candidate W bosons by minimising the difference between the hadronic and leptonic reconstructed T masses, $\Delta m_{\text{VLQ}} \equiv |m_T^{\text{lep}} - m_T^{\text{had}}|$. If the event contains one b-tagged jet, only combinations that include the b-tagged jet are considered. If the event contains two or more b-tagged jets, only combinations with the two b-tagged jets leading in p_{T} are considered. Signal events are expected to have VLQs with low p_{T} and high mass, causing the jet paired with the W_{had}, referred to as b_{had}, to be well separated from the W_{had}. By contrast, $t\bar{t}$ events will have high-p_{T} t-quarks that lead to a small opening angle between the resulting W and b. Therefore, a requirement of $\Delta R(W_{\text{had}}, b_{\text{had}}) > 1.0$ is imposed to reduce the $t\bar{t}$ background. Well reconstructed signal events should also have small values of Δm_{VLQ}, with both the reconstructed T-quark masses m_T^{lep} and m_T^{had} close to the actual mass of the T-quark. A similar statement can be made for $t\bar{t}$ events, but the reconstructed variables m_T^{lep} and m_T^{had} are close to the t-quark mass m_t. Production of $T\bar{T}$ events with other decays, such as $T \to Ht/Zt$, will tend to have m_T^{lep} and m_T^{had} near the T-quark mass, but with large values of Δm_{VLQ} as the VLQ reconstruction is less optimised for t-quarks from the T-quark decay. Detector effects, final state radiation, and mis-reconstruction can also broaden the reconstructed mass peaks for signal and $t\bar{t}$ events. In contrast, a smooth distribution in Δm_{VLQ} is expected for background processes, such as W+jets and single top production. The variable Δm_{VLQ} is therefore used to separate regions enriched in single top background with similar kinematic properties as the single top events in the signal region.

The scalar sum S_{T} of the p_{T} of the selected small-R jets, the lepton p_{T} and the $E_{\text{T}}^{\text{miss}}$, is a powerful discrimination quantity, due to the large expected mass of the T. The signal regions require $S_{\text{T}} > 1900$ GeV, while regions to constrain the background nuisance parameters and normalisations require $1400 < S_{\text{T}} < 1900$ GeV. The control and signal regions are further divided by Δm_{VLQ}, as illustrated in Fig. 2. Events in these regions are used in the final likelihood fit as described in Section 8. The signal region is defined by $S_{\text{T}} > 1900$ GeV and $\Delta m_{\text{VLQ}} < 500$ GeV, which is further divided into the regions SR1 with $\Delta m_{\text{VLQ}} < 200$ GeV and SR2 with $200 < \Delta m_{\text{VLQ}} < 500$ GeV. The region SR1 is designed to capture the best-reconstructed VLQ events that would have a narrow peak in the m_T^{lep} and m_T^{had} distributions. The region SR2 will capture less-well-reconstructed VLQ events, resulting in broader mass distributions. Despite this, the fraction of VLQs expected to enter this region is non-negligible. A control region with $S_{\text{T}} > 1900$ GeV and $\Delta m_{\text{VLQ}} > 500$ GeV, denoted $S_{\text{T}}^{\text{High}}\Delta m$CR, has low signal contamination for signal masses that are not excluded yet and is dominated by single top production. This control region provides an opportunity to constrain the modelling of the single top background using events with kinematic properties similar to the signal region. The region with $1400 < S_{\text{T}} < 1900$ GeV is divided into two control regions in Δm_{VLQ}: $t\bar{t}$CR with $\Delta m_{\text{VLQ}} < 500$ GeV and $S_{\text{T}}^{\text{Low}}\Delta m$CR with $\Delta m_{\text{VLQ}} > 500$ GeV. The $t\bar{t}$CR is rich in $t\bar{t}$ events with a purity of nearly 70%, allowing the constraint of the normalisation and modelling of t-quark pair production. The $S_{\text{T}}^{\text{Low}}\Delta m$CR provides a second region for constraining the single top background, but with kinematics properties similar to the $t\bar{t}$CR. A summary of all regions is provided in Table 1. The regions not included in the fit, W+jetsCR and $t\bar{t}$RWR ($t\bar{t}$ reweighting region), serve to derive data-driven corrections to the background modelling and are discussed in the following section.

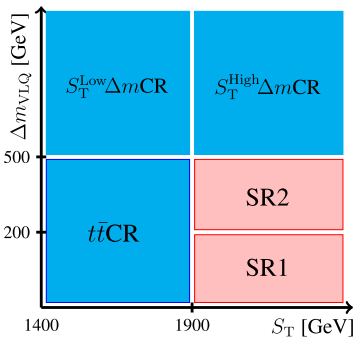

Fig. 2. Illustration of the two-dimensional plane in S_{T} and Δm_{VLQ} on which the signal and control regions, included in the final combined likelihood fit, are defined.

6. Background estimate

Contributions from the dominant background processes, $t\bar{t}$ and W+jets production, are estimated by using MC simulation with data-driven corrections derived in dedicated control regions dominated by the respective process. The SM backgrounds containing a prompt-lepton (single top, Z+jets, diboson, etc.) are also estimated by using MC simulations. Finally, the small contribution from multijet events is estimated by using a data-driven approach.

A correction for W+jets events is derived in a dedicated control region referred to as the W+jetsCR. This region is constructed to be orthogonal to the signal region, in particular with an inverted jet mass requirement in the hadronic W boson tagging algorithm. Possible biases in the modelling of W+jets events due to the inversion of this requirement are investigated and taken into account with a dedicated uncertainty, as detailed below. The W+jetsCR also requires $900 < S_{\text{T}} < 1900$ GeV to reduce possible contamination from VLQ signal events. All other selection requirements are the same as in the signal region, as shown in Table 1.

Requiring at least one b-tagged jet, similar to the signal region requirement, causes the W+jetsCR to have a significant contribution from $t\bar{t}$ events. This requirement helps to validate the correction to simulated W+jets events as the modelling of W+jets depends on the heavy-flavour requirement [82]. The estimate of the W+jets correction is based on the charge asymmetry of W+jets events in the W+jetsCR, present due to the asymmetry in u- and d-quark content in the proton [83]. Charge asymmetry is defined as $A = N_+ - N_-$, where N_+ and N_- are the numbers of events with a positively or negatively charged lepton, respectively. The correction factor to the W+jets normalisation is calculated by comparing A in data and MC simulation in the W+jetsCR. This approach decouples the charge-asymmetric process, W+jets, from possible mis-modelling of the $t\bar{t}$ events, which is a charge-symmetric process. This method is also useful for separating charge-asymmetric events from the VLQ signal, as it is also charge-symmetric. The contributions to A from charge-symmetric backgrounds, such as $t\bar{t}$ and multijet, cancel out. The small contributions from other charge-asymmetric backgrounds, such as single top, diboson, and t-associated production, is accounted for using MC samples. The dependence of the W+jets normalisation on S_{T} and the W-tag requirements was investigated in the control region sidebands (relaxed or tightened requirements on S_{T} or the W-tag selection in the W+jetsCR) to ensure applicability of this correction in the signal region. The W+jets correction is derived as a function of S_{T} up to $S_{\text{T}} = 4$ TeV as a check and no dependence of the W+jets correction on the event S_{T} is observed. An additional uncertainty is added to cover the difference between the normalisation correction found in the W+jetsCR and the control region sidebands with varied W-tag requirements. The dependence of the W+jets normalisation on other relevant event and kinematic variables is checked and no significant dependen-

Table 1
Overview of the signal and control regions used in the analysis.

Selection	SR1 / SR2	$t\bar{t}$CR	$S_{\mathrm{T}}^{\mathrm{Low}}\Delta m$CR / $S_{\mathrm{T}}^{\mathrm{High}}\Delta m$CR	W+jetsCR	$t\bar{t}$RWR
Preselection	✓	✓	✓	✓	✓
$N_{\text{Large-}R\text{ Jet}}$	≥ 1	≥ 1	≥ 1	≥ 1	≥ 1
S_{T} [GeV]	>1900	1400–1900	1400–1900 / >1900	900–1900	>800
$N_{W\text{-tag}}$	≥ 1	≥ 1	≥ 1	≥ 1 partially inverted	≥ 1
$N_{b\text{-tag}}$	≥ 1	≥ 1	≥ 1	≥ 1	≥ 2
$\Delta R(W_{\mathrm{had}}, b_{\mathrm{had}})$	> 1.0	> 1.0	> 1.0	–	< 1.0
$\Delta R(\ell, \nu)$	< 0.7	< 0.7	< 0.7	< 1.0	< 1.2
Δm_{VLQ} [GeV]	< 200 / 200–500	< 500	> 500	–	–
$m_T^{\mathrm{lep}}, m_T^{\mathrm{had}}$ [GeV]	–	–	–	–	< 700
Included in fit	yes / yes	yes	yes / yes	no	no
Goal	Optimise signal sensitivity	Constrain $t\bar{t}$ normalisation	Constrain single top uncertainties	Derive W + jets normalisation factor	Derive $t\bar{t}$ S_{T} shape reweighting

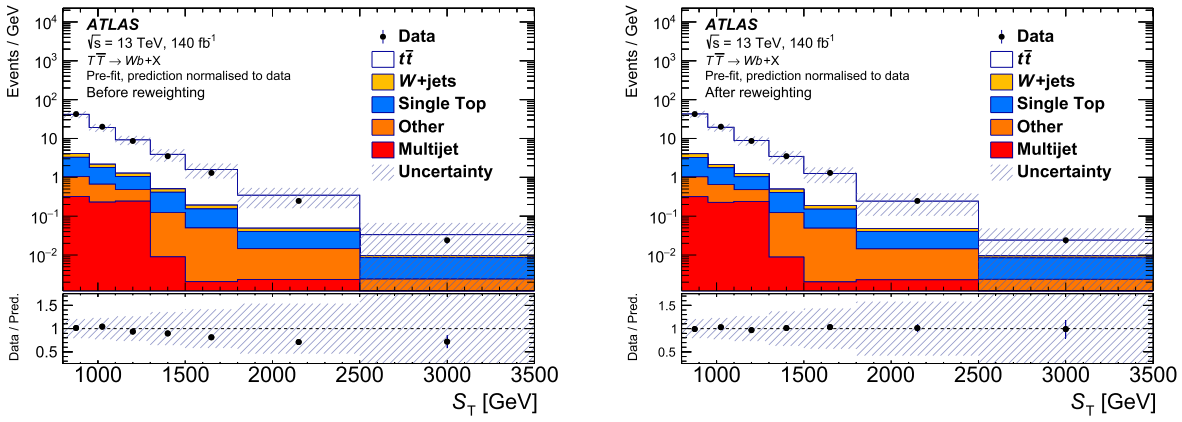

Fig. 3. Distributions of S_{T} for data (dots) and predictions (histograms with various colours) in the $t\bar{t}$RWR (a) before and (b) after applying the reweighting (see text). The prediction is normalised to the data to illustrate the discrepancies in the shape of the distribution and the effect of the S_{T} shape reweighting. The error bars include the statistical uncertainty and the shaded band represents the total systematic uncertainty. The last bin includes the overflow.

cies are observed. Thus, a single normalisation factor is applied to the W+jets MC prediction. The W+jets normalisation correction amounts to $f_{W+\mathrm{jets}} = 0.915 \pm 0.09$ (stat.) ± 0.54 (syst.), the largest systematic uncertainties are from the modelling of the single top background and from inverting the requirements of the W-tag selection.

The $t\bar{t}$ background estimate from MC simulation is known to overestimate the number of events at high t-quark p_{T} [84], directly impacting the modelling of S_{T}, which is essential for discriminating signal from background. Therefore, a data-driven reweighting is applied to the $t\bar{t}$ MC events to correct for the difference between the MC and the data in the S_{T} distribution. The correction is derived in the $t\bar{t}$ reweighting region $t\bar{t}$RWR, defined in Table 1, which has a $t\bar{t}$ purity of 89%, with the next most significant contribution from single top background at 6%. The main selection criteria differentiating the $t\bar{t}$RWR from the signal region are $\Delta R(W\text{-tag}, b_{\mathrm{had}}) < 1.0$ and $S_{\mathrm{T}} > 800$ GeV. These criteria are motivated by the low angular distance between the W boson and b-quark from the decay of a high-p_{T} t-quark. To ensure that the contamination by signal event in $t\bar{t}$RWR is low, the invariant masses of the reconstructed VLQs, m_T^{lep} and m_T^{had}, are required to be smaller than 700 GeV. Fig. 3(a) shows the S_{T} distributions in the $t\bar{t}$RWR before deriving the reweighting.

The reweighting is constructed to correct the shape of the S_{T} distribution, but not the normalisation, as it is varying freely in the final likelihood fit and ultimately constrained by the data in the $t\bar{t}$CR. The contributions to the $t\bar{t}$RWR from processes other than $t\bar{t}$ are subtracted from the data and the ratio of the resulting S_{T} distribution and the S_{T} distribution from the $t\bar{t}$ prediction is calculated. The correction factor is then derived in a fit to that ratio with a function of the form:

$$f(S_{\mathrm{T}}) = p_0 \cdot \exp\left(-p_1 \cdot (S_{\mathrm{T}} - p_2)^2\right) + p_3, \quad (1)$$

where p_i (with $i = 0, 1, 2, 3$) are the free parameters of the fit. Other functional forms are also studied, but the one in Eq. (1) is found to describe the data/MC ratio most accurately. The fit is also found to be consistent for different fit intervals and bin choices. The S_{T} and the jet multiplicity, N_{jets}, are correlated, so the correction to S_{T} could also depend on N_{jets}. Therefore, separate fits are performed for events with $3 \leq N_{\mathrm{jets}} \leq 6$ and $N_{\mathrm{jets}} \geq 7$. Fig. 3(b) shows the S_{T} distribution in the $t\bar{t}$RWR after the application of the reweighting correction.

The statistical uncertainty of the fit is propagated as an uncertainty on the reweighting correction. The impact of the uncertainty in the single top modelling is taken into account by varying the single top contribution by 100% in the $t\bar{t}$RWR region. Uncertainties in other processes have negligible impact on the extracted reweighting. The offset parameter p_3 in Eq. (1) causes the function to approach an asymptote at high values of S_{T} to 0.64 for $3 \leq N_{\mathrm{jets}} \leq 6$ and 0.62 for $N_{\mathrm{jets}} \geq 7$, where the statistical uncertainty is too large to determine the exact dependence of the correction on S_T with confidence. In addition, an uncertainty of 58% (38%), covering the large statistical uncertainty in the high-S_{T} tail, is added if $S_{\mathrm{T}} \geq 2.5$ TeV for events with $3 \leq N_{\mathrm{jets}} \leq 6$ ($N_{\mathrm{jets}} \geq 7$). Finally, the correction in S_{T} is tested in a dedicated $t\bar{t}$-dominated validation region, where the $t\bar{t}$ MC estimate is found to have good agreement with data after application of the S_{T}-dependent correction.

Events from multijet production satisfy the lepton requirement of the signal region by mis-identifying a hadronic jet as a lepton or a non-prompt lepton from a heavy-flavour jet, collectively referred to as non-prompt leptons. The contribution from multijet production is small, accounting for about 5% of the events in the signal region. Back-

ground from these processes is estimated by using a data-driven"Matrix Method" (MM) [85]. This method uses the classification of the leptons in "loose" and "tight" categories to predict the number of non-prompt leptons. Tight leptons correspond to signal leptons, as described in Section 5. Loose leptons satisfy the baseline criteria, as defined in Section 5, but fail to meet the tight lepton requirements. A "loose region" enriched in non-prompt leptons is created by changing the lepton requirement from tight to loose for the signal region selection. The number of events with prompt (non-prompt) leptons in the signal region is related to the number of events with prompt (non-prompt) leptons in the loose region by the efficiencies for prompt (non-prompt) leptons that satisfy the baseline lepton requirements to also satisfy the tight requirements, which is referred to as the "real efficiency" ("fake efficiency"). Therefore, once the real and fake efficiencies are determined, the number of events with non-prompt leptons (the multijet events) in the signal region can be calculated, as described in Ref. [86].

The tight lepton criteria reduce the contribution of the multijet background in the signal and control regions to very low levels, such that the shapes of differential distributions estimated by the MM are dominated by statistical fluctuations. An accurate prediction for the multijet background is particularly important for the m_T^{lep} distribution, as it is used in the final likelihood fit. As the background events do not contain real VLQ decays, the distribution of reconstructed masses is largely determined by the kinematic constraints from the event selection. As a result, the m_T^{lep} distribution for Z+jets and multijet events are very similar, but is much more stable for Z+jets. Therefore, in the final fit, the shape of the m_T^{lep} template for the multijet background is taken from Z+jets events, while the total predicted yield is determined from the MM calculation.

For reconstructed m_T^{lep} below 200 GeV, the MM estimate for multijet events is extremely sensitive to the amount of $t\bar{t}$ that is subtracted from the data. Therefore, an iterative method is employed to determine the total predicted multijet yield for the scaling of the Z+jets template. First, the MM prediction is evaluated using the nominal normalization for the subtracted $t\bar{t}$. Second, the m_T^{lep} template (taken from Z+jets events) is scaled to have the same yield as the MM prediction for events with $m_T^{\text{lep}} > 200$ GeV. Third, the normalisation of the $t\bar{t}$ events is adjusted to get the MM prediction to agree with the m_T^{lep} template for $m_T^{\text{lep}} > 200$ GeV. The second and third steps are then repeated until the predicted multijet yield changes by less than 1% from the previous iteration. An uncertainty of 100% is assigned to the multijet yield to account for the impact of systematic uncertainties in the modelling of prompt lepton processes and the fake-lepton efficiency. An additional uncorrelated uncertainty of 100% is applied to the multijet prediction for $m_T^{\text{lep}} < 200$ GeV to account for the uncertainty of the MM prediction in that region due to the normalization of the $t\bar{t}$ background. To model the multijet shape in other variables and analysis regions, the MC sample for multijet production, scaled to the MM estimate, is used.

7. Systematic uncertainties

Systematic uncertainties are broadly grouped into the following two classes: experimental uncertainties, which are related to the modelling of the detector response and reconstruction of physics objects, and to the data-driven background estimate or the data-driven corrections to the simulated backgrounds; and theoretical uncertainties, which are related to the modelling of the physics processes by simulation. Unless stated otherwise, uncertainties from a common source are correlated across processes and regions in the final statistical analysis and the impact of the uncertainties is allowed to be constrained by the likelihood fit to the data.

The largest systematic uncertainties are related to the modelling of $t\bar{t}$ and single top backgrounds. The uncertainties in the theory for the $t\bar{t}$ prediction include the choice of MC generator (in this case, MC events were generated to NLO accuracy); ISR, FSR, and parton shower model; and shower matching scheme of simulated $t\bar{t}$ events. Each of these uncertainties is evaluated by comparing the nominal $t\bar{t}$ prediction to the alternative MC samples, as described in Section 3. Modelling uncertainties in the single top prediction include the choice of the parton shower and the matching of the NLO matrix element to the parton shower, which are evaluated using alternative samples as described in Section 3. Similarly, an uncertainty due to the choice of the $t\bar{t}/Wt$ overlap removal scheme is evaluated by comparing the nominal single top MC produced with DR scheme to the alternative sample produced with the DS scheme [87]. The DR scheme is found to be more compatible with the data at lower energies, while at higher energies, the DS scheme is observed to provide a better description of the data. To avoid extrapolation of the DS versus DR uncertainty from the regions defined with low S_{T} to those at high S_{T}, this uncertainty is split into a high-S_{T} component, applied to regions with $S_{\text{T}} > 1.9$ TeV, and a low-S_{T} component, applied to regions with $1.4 < S_{\text{T}} < 1.9$ TeV. For both the single top and the $t\bar{t}$ production, uncertainties in the PDF are obtained using the `PDF4LHC15` combined PDF set [88]. The effect of QCD scale uncertainties is estimated by independently doubling or halving the renormalisation and factorisation scales for single top and $t\bar{t}$ production, respectively. The QCD scale variation with the largest impact on the fit discriminant (m_T^{lep}) is used.

To simplify the statistical analysis, all the smaller backgrounds from $t\bar{t}V$, Z+jets, rare top processes and diboson production are grouped into a single category named "other", and a single overall normalisation uncertainty of 50% is applied. This uncertainty of 50% is adopted from the uncertainty in Z+jets events which has the largest relative uncertainty among the processes contained in the "other" category. The uncertainty in the Z+jets contribution was estimated in the previous analysis [13] by investigating the mis-modelling of the jet multiplicity of Z+jets events.

Experimental uncertainties include an uncertainty of 0.83% on the integrated luminosity measurement on the combined 2015−2018 data [22], obtained using the LUCID-2 detector [23] for the primary luminosity measurements. Uncertainties in leptons arise from potential mis-modelling of the electron and muon energy scales and resolutions [62,64] and from uncertainties in the correction factors to the electron and muon trigger, reconstruction, identification and isolation efficiencies [62,63].

Small-R jets have uncertainties in the JES, the JER [68] and on the JMS [77]. An uncertainty is assigned to the JVT selection efficiency [69] and to the reweighting factors that correct the pile-up profile in MC simulations to match that in data. Similarly, JES, JER [77] and JMS uncertainties, and in addition JMR [78] systematic uncertainties are assigned to large-radius jets. An uncertainty related to the scale and resolution of the track soft term in the $E_{\text{T}}^{\text{miss}}$ calculation [74] is applied.

Uncertainties in the b-tagging algorithm selection efficiency include uncertainties in the b-jet selection efficiency, c-jet and light jet mistag rate correction factors and additional components from the extrapolation of the calibrations to high p_{T} and from c-jets to τ leptons [71–73]. An uncertainty is assigned to the efficiency correction of the W boson tagging algorithm [79,81].

Uncertainties in the data-driven corrections for simulated backgrounds or in the data-driven multijet event estimate are briefly listed below and detailed in Section 6. The uncertainty in the data-driven correction for simulated W+jets events is 60%. This is among the dominant systematic uncertainties, though still much smaller than the statistical uncertainty of the data set. The uncertainty in the $t\bar{t}$ S_{T} shape reweighting consists of a statistical component and a systematic component from the uncertainty in the single top contribution in the $t\bar{t}$RWR. The two components affecting the multijet background estimate include a global 100% uncertainty in the MM estimate and an additional 100% uncertainty for reconstructed VLQ invariant masses m_T^{lep} below 200 GeV.

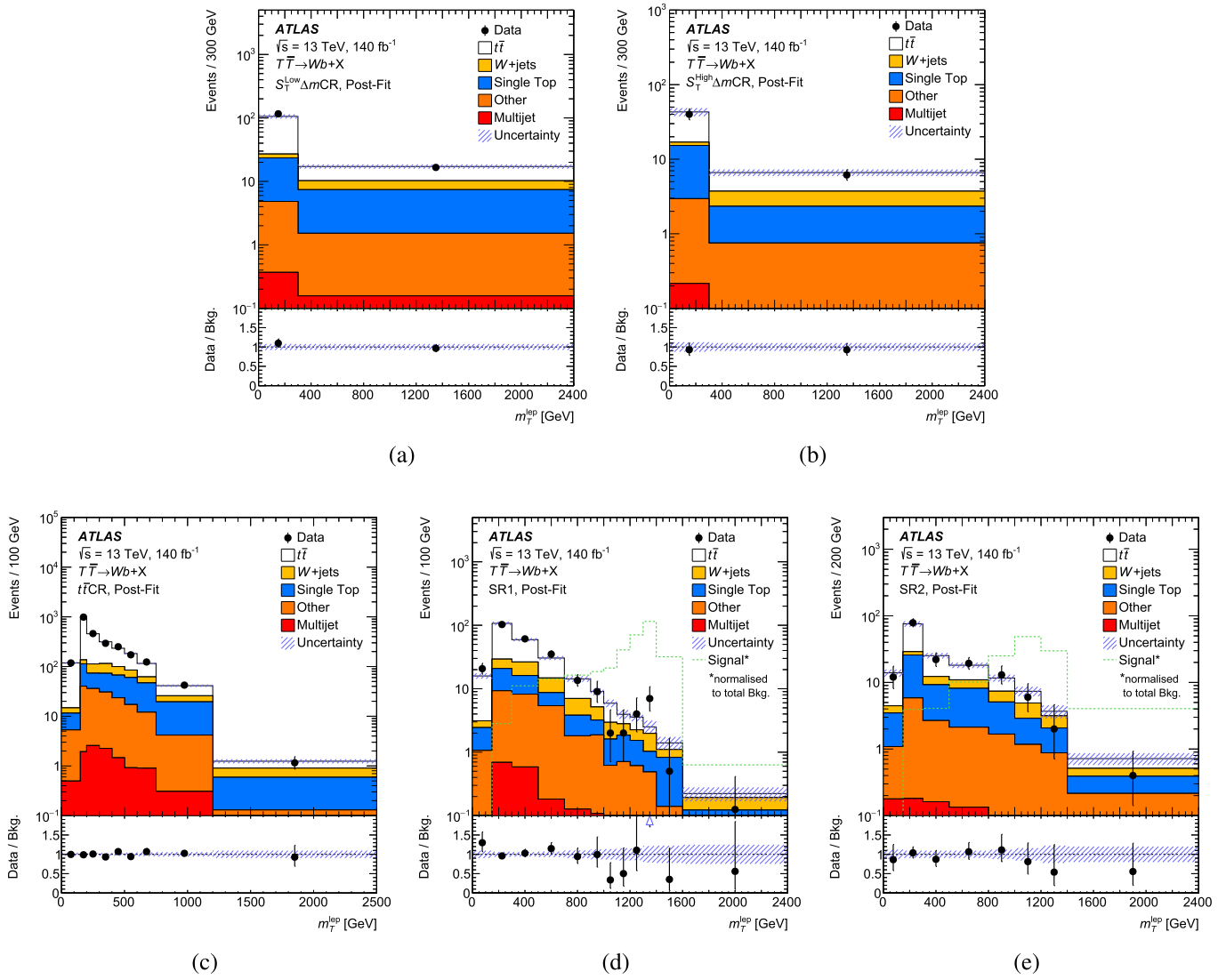

Fig. 4. Distribution for m_T^{lep} for data (dots) and predictions (histograms with various colours) in the five fit regions ((a) $S_{\text{T}}^{\text{Low}}\Delta m$CR, (b) $S_{\text{T}}^{\text{High}}\Delta m$CR, (c) $t\bar{t}$CR, (d) SR1, and (e) SR2, respectively) after the simultaneous fit to data under the background-only hypothesis (Post-Fit). The binning in m_T^{lep} was optimised to maximise the sensitivity to the signal in the signal regions while it is ensured that each bin of the fit regions contains a reasonable number of data events to guarantee good fit behaviour. The lower panel of each plot shows the ratio of data and predicted background yields. The arrow indicates that the ratio point is outside the ordinate range. The overflow events are included in the last bin. The error bars include the statistical uncertainty and the shaded band represents the systematic uncertainty after the likelihood fit (see text). The dashed green histograms in (d) SR1 and (e) SR2 show the shape for the signal with $m_{\text{VLQ}} = 1400\,\text{GeV}$ and $\mathcal{B}(T \to Wb) = 1$ scaled to the total background prediction. The expected signal event yields in each of the fit regions are displayed in Table 3.

8. Statistical analysis and results

The presence of the VLQ signal is tested by using a fit to the reconstructed mass distributions of the leptonically decaying T candidate (m_T^{lep}) from the signal regions SR1 and SR2 and control regions $t\bar{t}$CR, $S_{\text{T}}^{\text{Low}}\Delta m$CR, and $S_{\text{T}}^{\text{High}}\Delta m$CR, denoted fit regions. The mass of the leptonically decaying T-quark is chosen because it is found to have a better resolution and sensitivity than the mass of the hadronically decaying T-quark. The fit maximises a binned likelihood function, $\mathcal{L}(\mu, \theta)$, constructed as a product of Poisson probabilities for all bins considered in the search and depends on the parameter of interest μ and a vector of nuisance parameters (NP) θ. The parameter of interest is the signal strength $\mu = \sigma^{\text{test}}/\sigma^{\text{theory}}$, where σ^{test} is the value for the VLQ cross-section being tested and σ^{theory} is the theoretical prediction. Each NP θ_i encodes a systematic uncertainty with a Gaussian function prior, except the normalisations of the $t\bar{t}$ and single top backgrounds, which are unconstrained, and the statistical uncertainties due to the finite size of the MC samples, which are included as one additional NP per bin that accounts for the statistical uncertainty of the total estimated yield in the

Table 2
Event yields in the five fit regions after the fit to the data under the background-only hypothesis. The uncertainties include statistical and systematic uncertainties. The uncertainties in the individual background components can be larger than the uncertainty in the sum of the backgrounds due to correlations.

	SR1	SR2	$S_{\text{T}}^{\text{High}}\Delta m$CR	$t\bar{t}$CR	$S_{\text{T}}^{\text{Low}}\Delta m$CR
$t\bar{t}$	257 ±33	74 ±14	46 ±9	1513 ±150	127 ±18
W+jets	61 ±25	17 ±7	12 ±5	213 ±90	24 ±10
Single Top	53 ±19	40 ±14	23 ±10	340 ±120	60 ±20
Other	48 ±21	15 ±7	7.5 ±3.4	160 ±70	14 ±6
Multijet	3 ±11	0.9 ±3.1	0.7 ±2.4	10 ±40	1 ±5
Total	422 ±21	146 ±11	89 ±8	2240 ±60	226 ±13
Data	430	142	83	2235	232

Table 3
Expected $T\bar{T}$ event yields in the five fit regions for various VLQ scenarios. The uncertainties include statistical and systematic uncertainties.

Yields for $\mathcal{B}(T \to Wb) = 1$:					
m_{VLQ}/GeV	SR1	SR2	$S_{\mathrm{T}}^{\mathrm{High}}\Delta m$CR	$t\bar{t}$CR	$S_{\mathrm{T}}^{\mathrm{Low}}\Delta m$CR
1200	83 ±4	26.9 ±1.3	9.5 ±0.6	18.7 ±0.6	1.65 ±0.11
1400	27.6 ±1.7	10.6 ±0.7	4.6 ±0.4	2.41 ±0.10	0.24 ±0.04
1600	8.6 ±0.6	3.59 ±0.24	1.87 ±0.14	0.273 ±0.017	0.066 ±0.009
1800	2.69 ±0.23	1.47 ±0.11	0.81 ±0.06	0.057 ±0.006	0.0076 ±0.0015
Yields for SU(2) singlet T:					
m_{VLQ}/GeV	SR1	SR2	$S_{\mathrm{T}}^{\mathrm{High}}\Delta m$CR	$t\bar{t}$CR	$S_{\mathrm{T}}^{\mathrm{Low}}\Delta m$CR
1200	42.9 ±2.1	20.4 ±1.2	9.8 ±0.8	12.5 ±0.5	1.49 ±0.08
1400	14.8 ±0.9	7.7 ±0.5	4.2 ±0.4	1.71 ±0.08	0.267 ±0.024
1600	4.66 ±0.32	2.58 ±0.18	1.82 ±0.16	0.246 ±0.013	0.057 ±0.004
1800	1.53 ±0.13	0.94 ±0.07	0.75 ±0.06	0.0526 ±0.0023	0.0101 ±0.0007

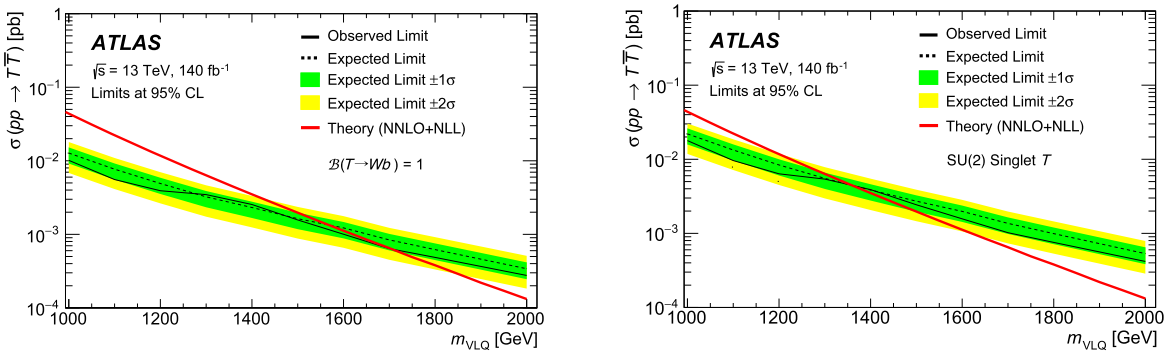

Fig. 5. Expected (dashed black line) and observed (solid black line) upper limits at the 95% CL on the $T\bar{T}$ cross-section as a function of T-quark mass for (a) the $\mathcal{B}(T \to Wb) = 1$ scenario and (b) in the SU(2) singlet T scenario. The green and yellow bands correspond to ±1 and ±2 standard deviations around the expected limit, respectively. The thin red line shows the theoretical prediction.

given bin. If an uncertainty would impact the normalisation or shape of all bins for a given process by less than 1%, the NP is removed from the fit for that process. The test statistic q_μ is defined as the profile likelihood ratio, $q_\mu = -2\ln(\mathcal{L}(\mu, \hat{\hat{\theta}}_\mu)/\mathcal{L}(\hat{\mu}, \hat{\theta}))$, where $\hat{\mu}$ and $\hat{\theta}$ are the values of the parameters that maximise the likelihood function (with the constraint $0 \leq \hat{\mu} \leq \mu$), and $\hat{\hat{\theta}}_\mu$ are the values of the nuisance parameters that maximise the likelihood function for a given value of μ. The compatibility with the background-only hypothesis for the observed data is tested by setting $\mu = 0$ in the profile likelihood ratio. Upper limits on the cross-section times branching ratio for a given signal are derived by using q_μ in the modified frequentist $\mathrm{CL_s}$ method [89,90], approximated using the asymptotic formulae [91]. For a given signal, the cross-section times branching ratio is excluded at ≥ 95% confidence level (CL) when $\mathrm{CL_s} < 0.05$.

Fig. 4 shows the m_T^{lep} distribution in each of the five fit regions after the simultaneous fit to the background-only hypothesis to data. The m_T^{lep} distributions of the SM backgrounds show a steep decline towards high m_T^{lep}, whereas the signal m_T^{lep} distribution is expected to peak close to the simulated m_{VLQ}, at high m_T^{lep} in SR1 and SR2, effectively distinguishing it from the SM backgrounds. The corresponding event yields are listed in Table 2. The uncertainty in the total prediction does not equal the sum in quadrature of the individual component due to correlations between the fit parameters. The expected number of $T\bar{T}$ signal events in each of the five fit regions are given in Table 3 for various VLQ scenarios. The compatibility with the background-only hypothesis for the data is estimated by integrating the distribution of the test statistic above the observed value of q_0. This value is computed for each signal scenario considered, defined by the assumed mass of the T-quark and the three decay branching ratios. These results assume the T-quark has a narrow width.

No significant excess above the background expectation is found. Upper limits at the 95% CL on the $T\bar{T}$ production cross-section are set for two benchmark scenarios as a function of T-quark mass m_{VLQ} and compared with the theoretical prediction from Top++ 2.0 (see Fig. 5). The resulting lower limit on m_{VLQ} is determined using the central value of the theoretical cross-section prediction.

For $\mathcal{B}(T \to Wb) = 1$ and T-quark masses from 1000 GeV to 2000 GeV, $T\bar{T}$ production cross-sections greater than 10.1 fb to 0.27 fb are excluded at 95% CL. Comparing to the theory cross-section, this results in an observed (expected) lower limit on the T-quark mass of m_{VLQ} >1700 GeV (1570 GeV) for this scenario. For branching ratios corresponding to the SU(2) singlet T scenario, the observed (expected) 95% CL lower mass limit is m_{VLQ} >1360 GeV (1360 GeV). The sensitivity of the analysis is limited by the statistical uncertainty in the data sample size. Including all systematic uncertainties for the $\mathcal{B}(T \to Wb) = 1$ scenario degrades the expected cross-section limit by less than 3.7% for any of the tested masses, and reduces the expected mass limit by only 10 GeV.

In the signal region, the prediction is found to slightly overestimate the data in the signal-sensitive high mass tail of the m_T^{lep} distribution. Therefore, the observed limits on the signal cross-section, and thus also on the signal mass m_{VLQ}, are generally more stringent than the expected limits. Large bin-to-bin variations between 1000 to 1600 GeV in the m_T^{lep} distribution are observed in SR1, with an excess relative to the prediction in one bin and deficits in three bins. However, no signal model is compatible with the narrow excess in SR1, as the width of the m_T^{lep} distribution for any of the signal models would be much wider than

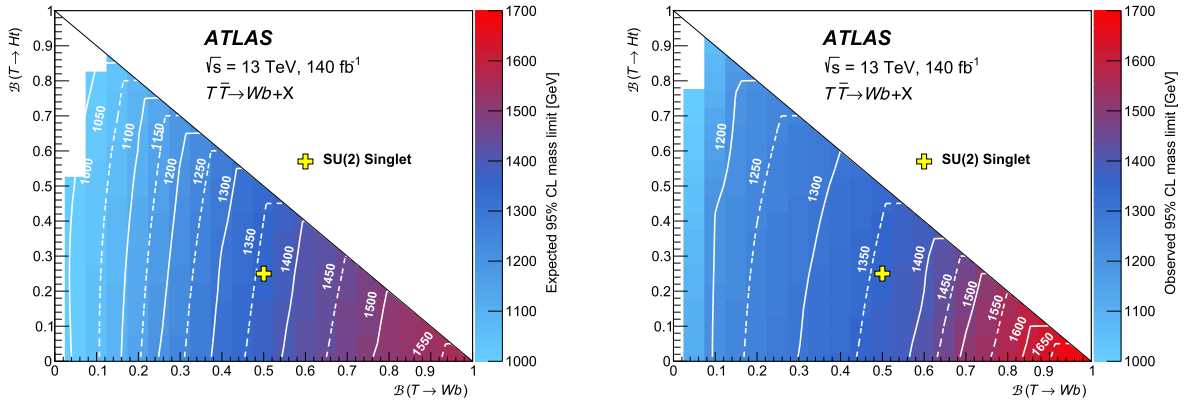

Fig. 6. (a) Expected and (b) observed 95% CL lower limits on the mass of the T-quark in the branching-ratio plane of $\mathcal{B}(T \to Wb)$ versus $\mathcal{B}(T \to Ht)$. Contour lines are provided to guide the eye. The white region is due to the lower mass limit falling below 1000 GeV, the lowest signal mass considered in this search. The yellow marker indicates the branching ratio for the SU(2) singlet B scenario.

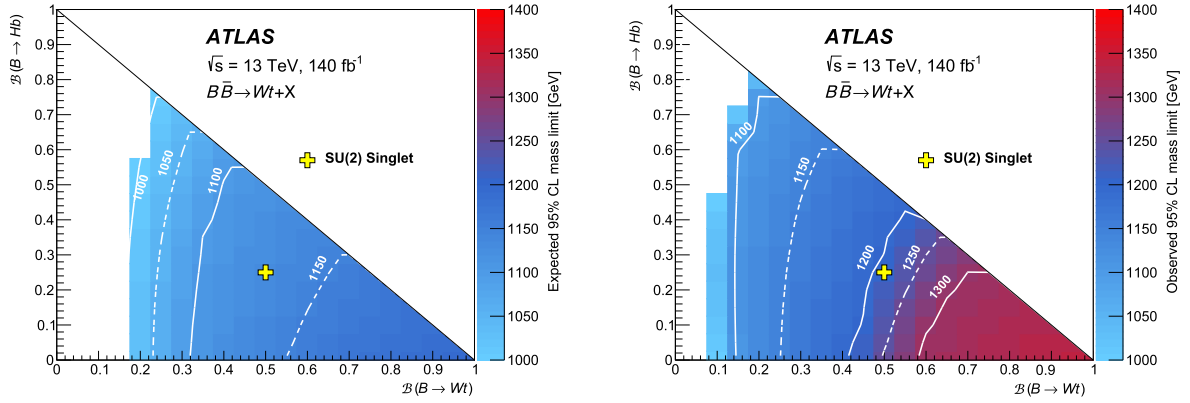

Fig. 7. (a) Expected and (b) observed 95% CL lower limits on the mass of the B-quark in the branching-ratio plane of $\mathcal{B}(B \to Wt)$ versus $\mathcal{B}(B \to Hb)$. Contour lines are provided to guide the eye. The white region is due to the lower mass limit falling below 1000 GeV, the lowest signal mass considered in this search. The yellow marker indicates the branching ratio for the SU(2) singlet B scenario.

the observed one-bin excess. Additionally, no such excess or large bin-to-bin variations of the data are observed in SR2. The narrow excess in SR1 does lead to weaker observed cross-section limits in an m_{VLQ} interval between around 1250 GeV to 1500 GeV relative to the rest of the m_{VLQ} spectrum.

In the previous search by ATLAS performed on a fraction of this data set with an integrated luminosity of 36 fb^{-1} [13], observed (expected) 95% CL mass limits of 1350 GeV (1310 GeV) for the scenario $\mathcal{B}(T \to Wb) = 1$ and 1170 GeV (1080 GeV) for a singlet T were found. The present search thus extends the observed mass limits by 350 GeV and 190 GeV for the $\mathcal{B}(T \to Wb) = 1$ and singlet T case, respectively. The increase of the mass limits can almost entirely be attributed to the increase in the size of the data sample from 36 fb^{-1} to 140 fb^{-1}, but about 15% (20%) of the improvement on the mass limits for the $\mathcal{B}(T \to Wb) = 1$ (singlet T) scenario is expected to come from changes in the analysis strategy, especially from improvements to the W boson tagging and the slicing of the signal region into two regions, SR1 and SR2 according to Δm_{VLQ}.

To check that the results do not depend on the weak-isospin of the T-quark in the simulated signal events, a sample of $T\bar{T}$ events with a mass of 1.2 TeV was generated for an SU(2) doublet T-quark and compared with the nominal sample of the same mass generated with an SU(2) singlet T-quark. Both the expected number of events and expected excluded cross-section are consistent between the two samples. Thus the limits obtained are also applicable to VLQ models with non-zero weak-isospin. As there is no explicit use of charge identification, the $\mathcal{B}(T \to Wb) = 1$ limits are applicable to the pair-production of vector-like Y-quarks of charge $-4/3$, which decay exclusively into Wb.

In addition to the benchmark scenarios, other combinations of T branching ratios are tested by reweighting the relative contributions of the three T-quark decay modes. Fig. 6 shows the expected and observed lower limits on the T-quark mass as a function of $\mathcal{B}(T \to Wb)$ and $\mathcal{B}(T \to Ht)$. For each point in the figure, the branching ratios for $T \to Zt$ decay are determined by the requirement $\mathcal{B}(T \to Wb) + \mathcal{B}(T \to Ht) + \mathcal{B}(T \to Zt) = 1$. Although the analysis is designed to search for $T\bar{T}$, it also has sensitivity to $B\bar{B}$ production. Fig. 7 shows the expected and observed lower limits on the B-quark mass as a function of $\mathcal{B}(B \to Wt)$ and $\mathcal{B}(B \to Hb)$, with $\mathcal{B}(B \to Zb) = 1 - \mathcal{B}(B \to Wt) - \mathcal{B}(B \to Hb)$. For the $\mathcal{B}(B \to Wt) = 1$ case, a lower limit on the B-quark mass of 1345 GeV (1196 GeV) is observed (expected). Similarly to the $\mathcal{B}(T \to Wb) = 1$ case, the $\mathcal{B}(B \to Wt) = 1$ limits are applicable to the pair-production of vector-like X-quarks.

9. Conclusion

Pair-produced vector-like T-quarks are searched for in events with exactly one electron or muon, missing transverse momentum and jets using the full Run 2 ATLAS data set. Final states compatible with the decay of a pair of heavy vector-like quarks are selected and a combined fit to the mass of the reconstructed vector-like quark in three control

regions and two signal regions is made. No significant excess over the background expectation is observed and 95% CL upper limits are set on the vector-like quark cross-section and lower bounds are set on the vector-like quark mass. The search is optimised for $T\bar{T} \to WbWb$, thus the most stringent limits are set for $\mathcal{B}(T \to Wb) = 1$. For this scenario, masses below 1700 GeV (1570 GeV) are observed (expected) to be excluded at 95% CL, which is the current strongest limit for this production and decay mode. The limits for $\mathcal{B}(T \to Wb) = 1$ also apply to a vector-like Y-quark with charge $-4/3$, which decays exclusively into Wb. The observed (expected) lower mass limit for the weak isospin singlet T model is 1360 GeV (1360 GeV) and limits for other T-quark branching ratios are presented in the plane of $\mathcal{B}(T \to Wb)$ vs. $\mathcal{B}(T \to Ht)$. The analysis was also used to set limits on the mass of B-quarks as a function of branching ratios. This search improves the previous result that used 36 fb^{-1} of ATLAS data by 350 GeV for the scenario $\mathcal{B}(T \to Wb) = 1$ and by 190 GeV in the T singlet case.

Declaration of competing interest

The authors declare that they have no known competing financial interests or personal relationships that could have appeared to influence the work reported in this paper.

Data availability

The data for this manuscript are not available. The values in the plots and tables associated to this article are stored in HEPDATA (https://hepdata.cedar.ac.uk)

Acknowledgements

We thank CERN for the very successful operation of the LHC and its injectors, as well as the support staff at CERN and at our institutions worldwide without whom ATLAS could not be operated efficiently.

The crucial computing support from all WLCG partners is acknowledged gratefully, in particular from CERN, the ATLAS Tier-1 facilities at TRIUMF/SFU (Canada), NDGF (Denmark, Norway, Sweden), CC-IN2P3 (France), KIT/GridKA (Germany), INFN-CNAF (Italy), NL-T1 (Netherlands), PIC (Spain), RAL (UK) and BNL (USA), the Tier-2 facilities worldwide and large non-WLCG resource providers. Major contributors of computing resources are listed in Ref. [92].

We gratefully acknowledge the support of ANPCyT, Argentina; YerPhI, Armenia; ARC, Australia; BMWFW and FWF, Austria; ANAS, Azerbaijan; CNPq and FAPESP, Brazil; NSERC, NRC and CFI, Canada; CERN; ANID, Chile; CAS, MOST and NSFC, China; Minciencias, Colombia; MEYS CR, Czech Republic; DNRF and DNSRC, Denmark; IN2P3-CNRS and CEA-DRF/IRFU, France; SRNSFG, Georgia; BMBF, HGF and MPG, Germany; GSRI, Greece; RGC and Hong Kong SAR, China; ISF and Benoziyo Center, Israel; INFN, Italy; MEXT and JSPS, Japan; CNRST, Morocco; NWO, Netherlands; RCN, Norway; MEiN, Poland; FCT, Portugal; MNE/IFA, Romania; MESTD, Serbia; MSSR, Slovakia; ARRS and MIZŠ, Slovenia; DSI/NRF, South Africa; MICINN, Spain; SRC and Wallenberg Foundation, Sweden; SERI, SNSF and Cantons of Bern and Geneva, Switzerland; MOST, Taipei; TENMAK, Türkiye; STFC, United Kingdom; DOE and NSF, United States of America.

Individual groups and members have received support from BCKDF, Canarie, CRC and DRAC, Canada; CERN-CZ, PRIMUS 21/SCI/017 and UNCE SCI/013, Czech Republic; COST, ERC, ERDF, Horizon 2020, ICSC-NextGenerationEU and Marie Skłodowska-Curie Actions, European Union; Investissements d'Avenir Labex, Investissements d'Avenir Idex and ANR, France; DFG and AvH Foundation, Germany; Herakleitos, Thales and Aristeia programmes co-financed by EU-ESF and the Greek NSRF, Greece; BSF-NSF and MINERVA, Israel; Norwegian Financial Mechanism 2014-2021, Norway; NCN and NAWA, Poland; La Caixa Banking Foundation, CERCA Programme Generalitat de Catalunya and PROMETEO and GenT Programmes Generalitat Valenciana, Spain; Göran Gustafssons Stiftelser, Sweden; The Royal Society and Leverhulme Trust, United Kingdom.

In addition, individual members wish to acknowledge support from CERN: European Organization for Nuclear Research (CERN PJAS); Chile: Agencia Nacional de Investigación y Desarrollo (FONDECYT 1190886, FONDECYT 1210400, FONDECYT 1230812, FONDECYT 1230987); China: National Natural Science Foundation of China (NSFC - 12175119, NSFC 12275265, NSFC-12075060); Czech Republic: PRIMUS Research Programme (PRIMUS/21/SCI/017); European Union: European Research Council (ERC - 948254), Horizon 2020 Framework Programme (MUCCA - CHIST-ERA-19-XAI-00), European Union, Future Artificial Intelligence Research (FAIR-NextGenerationEU PE00000013), Italian Center for High Performance Computing, Big Data and Quantum Computing (ICSC, NextGenerationEU), Marie Sklodowska-Curie Actions (EU H2020 MSC IF GRANT NO 101033496); France: Agence Nationale de la Recherche (ANR-20-CE31-0013, ANR-21-CE31-0013, ANR-21-CE31-0022), Investissements d'Avenir Idex (ANR-11-LABX-0012), Investissements d'Avenir Labex (ANR-11-LABX-0012); Germany: Baden-Württemberg Stiftung (BW Stiftung-Postdoc Eliteprogramme), Deutsche Forschungsgemeinschaft (DFG - 469666862, DFG - CR 312/5-1); Italy: Istituto Nazionale di Fisica Nucleare (FELLINI G.A. n. 754496, ICSC, NextGenerationEU); Japan: Japan Society for the Promotion of Science (JSPS KAKENHI Grant No. 22KK0227, JSPS KAKENHI JP21H05085, JSPS KAKENHI JP22H01227, JSPS KAKENHI JP22H04944); Netherlands: Netherlands Organisation for Scientific Research (NWO Veni 2020 - VI.Veni.202.179); Norway: Research Council of Norway (RCN-314472); Poland: Polish National Agency for Academic Exchange (PPN/PPO/2020/1/00002/U/00001), Polish National Science Centre (NCN 2021/42/E/ST2/00350, NCN OPUS nr 2022/47/B/ST2/03059, NCN UMO-2019/34/E/ST2/00393, UMO-2020/37/B/ST2/01043, UMO-2021/40/C/ST2/00187); Slovenia: Slovenian Research Agency (ARIS grant J1-3010); Spain: BBVA Foundation (LEO22-1-603), Generalitat Valenciana (Artemisa, FEDER, IDIFEDER/2018/048), La Caixa Banking Foundation (LCF/BQ/PI20/11760025), Ministry of Science and Innovation (MCIN & NextGenEU -PCI2022-135018-2, MICIN & FEDER -PID2021-125273NB, RYC2019-028510-I, RYC2020-030254-I, RYC2021-031273-I, RYC2022-038164-I), PROMETEO and GenT Programmes Generalitat Valenciana (CIDEGENT/2019/023, CIDEGENT/2019/027); Sweden: Swedish Research Council (VR 2018-00482, VR 2022-03845, VR 2022-04683, VR grant 2021-03651), Knut and Alice Wallenberg Foundation (KAW 2017.0100, KAW 2018.0157, KAW 2018.0458, KAW 2019.0447); Switzerland: Swiss National Science Foundation (SNSF - PCEFP2_194658); United Kingdom: Leverhulme Trust (Leverhulme Trust RPG-2020-004); United States of America: Neubauer Family Foundation.

References

[1] L. Susskind, Dynamics of spontaneous symmetry breaking in the Weinberg-Salam theory, Phys. Rev. D 20 (1979) 2619.
[2] L. Randall, R. Sundrum, Large mass hierarchy from a small extra dimension, Phys. Rev. Lett. 83 (1999) 3370, arXiv:hep-ph/9905221.
[3] D.B. Kaplan, H. Georgi, S. Dimopoulos, Composite Higgs scalars, Phys. Lett. B 136 (1984) 187.
[4] N. Vignaroli, Discovering the composite Higgs through the decay of a heavy fermion, J. High Energy Phys. 07 (2012) 158, arXiv:1204.0468 [hep-ph].
[5] M. Schmaltz, D. Tucker-Smith, Little Higgs theories, Annu. Rev. Nucl. Part. Sci. 55 (2005) 229, arXiv:hep-ph/0502182.
[6] J.A. Aguilar-Saavedra, R. Benbrik, S. Heinemeyer, M. Pérez-Victoria, Handbook of vectorlike quarks: mixing and single production, Phys. Rev. D 88 (2013) 094010, arXiv:1306.0572 [hep-ph].
[7] O. Eberhardt, et al., Impact of a Higgs boson at a mass of 126 GeV on the standard model with three and four fermion generations, Phys. Rev. Lett. 109 (2012) 241802, arXiv:1209.1101 [hep-ph].
[8] ATLAS Collaboration, Combination of the searches for pair-produced vector-like partners of the third-generation quarks at $\sqrt{s} = 13\,TeV$ with the ATLAS detector, Phys. Rev. Lett. 121 (2018) 211801, arXiv:1808.02343 [hep-ex].
[9] ATLAS Collaboration, Search for pair-produced vector-like top and bottom partners in events with large missing transverse momentum in pp collisions with the ATLAS detector, Eur. Phys. J. C 83 (2023) 719, arXiv:2212.05263 [hep-ex].

[10] ATLAS Collaboration, Search for pair-production of vector-like quarks in pp collision events at $\sqrt{s} = 13$ TeV with at least one leptonically decaying Z boson and a third-generation quark with the ATLAS detector, Phys. Lett. B 843 (2023) 138019, arXiv:2210.15413 [hep-ex].

[11] CMS Collaboration, A search for bottom-type, vector-like quark pair production in a fully hadronic final state in proton–proton collisions at $\sqrt{s} = 13\,TeV$, Phys. Rev. D 102 (2020) 112004, arXiv:2008.09835 [hep-ex].

[12] CMS Collaboration, Search for pair production of vector-like quarks in leptonic final states in proton-proton collisions at $\sqrt{s} = 13$ TeV, J. High Energy Phys. 07 (2023) 020, arXiv:2209.07327 [hep-ex].

[13] ATLAS Collaboration, Search for pair production of heavy vector-like quarks decaying to high-p_T W bosons and b quarks in the lepton-plus-jets final state in pp collisions at $\sqrt{s} = 13\,TeV$ with the ATLAS detector, J. High Energy Phys. 10 (2017) 141, arXiv:1707.03347 [hep-ex].

[14] ATLAS Collaboration, Search for single production of vector-like T quarks decaying into Ht or Zt in pp collisions at $\sqrt{s} = 13$ TeV with the ATLAS detector, J. High Energy Phys. 08 (2023) 153, arXiv:2305.03401 [hep-ex].

[15] ATLAS Collaboration, Search for single production of a vectorlike T quark decaying into a Higgs boson and top quark with fully hadronic final states using the ATLAS detector, Phys. Rev. D 105 (2022) 092012, arXiv:2201.07045 [hep-ex].

[16] CMS Collaboration, Search for single production of a vector-like T quark decaying to a top quark and a Z boson in the final state with jets and missing transverse momentum at $\sqrt{s} = 13\,TeV$, J. High Energy Phys. 05 (2022) 093, arXiv:2201.02227 [hep-ex].

[17] CMS Collaboration, Search for a heavy resonance decaying into a top quark and a W boson in the lepton+jets final state at $\sqrt{s} = 13\,TeV$, J. High Energy Phys. 04 (2022) 048, arXiv:2111.10216 [hep-ex].

[18] CMS Collaboration, Search for a vector-like quark $T' \to tH$ via the diphoton decay mode of the Higgs boson in proton-proton collisions at $\sqrt{s} = 13$ TeV, J. High Energy Phys. 09 (2023) 057, arXiv:2302.12802 [hep-ex].

[19] A. Roy, N. Nikiforou, N. Castro, T. Andeen, Novel interpretation strategy for searches of singly produced vectorlike quarks at the LHC, Phys. Rev. D 101 (2020) 115027, arXiv:2003.00640 [hep-ph].

[20] ATLAS Collaboration, The ATLAS experiment at the CERN Large Hadron Collider, J. Instrum. 3 (2008) S08003.

[21] ATLAS Collaboration, The ATLAS collaboration software and firmware, ATL-SOFT-PUB-2021-001, https://cds.cern.ch/record/2767187, 2021.

[22] ATLAS Collaboration, Luminosity determination in pp collisions at $\sqrt{s} = 13$ TeV using the ATLAS detector at the LHC, Eur. Phys. J. C 83 (2023) 982, arXiv:2212.09379 [hep-ex].

[23] G. Avoni, et al., The new LUCID-2 detector for luminosity measurement and monitoring in ATLAS, J. Instrum. 13 (2018) P07017.

[24] ATLAS Collaboration, Performance of electron and photon triggers in ATLAS during LHC Run 2, Eur. Phys. J. C 80 (2020) 47, arXiv:1909.00761 [hep-ex].

[25] ATLAS Collaboration, Performance of the ATLAS muon triggers in Run 2, J. Instrum. 15 (2020) P09015, arXiv:2004.13447 [physics.ins-det].

[26] ATLAS Collaboration, Performance of the missing transverse momentum triggers for the ATLAS detector during Run-2 data taking, J. High Energy Phys. 08 (2020) 080, arXiv:2005.09554 [hep-ex].

[27] ATLAS Collaboration, ATLAS data quality operations and performance for 2015–2018 data-taking, J. Instrum. 15 (2020) P04003, arXiv:1911.04632 [physics.ins-det].

[28] ATLAS Collaboration, The ATLAS simulation infrastructure, Eur. Phys. J. C 70 (2010) 823, arXiv:1005.4568 [physics.ins-det].

[29] S. Agostinelli, et al., Geant4 – a simulation toolkit, Nucl. Instrum. Methods A 506 (2003) 250.

[30] ATLAS Collaboration, The simulation principle and performance of the ATLAS fast calorimeter simulation FastCaloSim, ATL-PHYS-PUB-2010-013, https://cds.cern.ch/record/1300517, 2010.

[31] T. Sjöstrand, et al., An introduction to PYTHIA 8.2, Comput. Phys. Commun. 191 (2015) 159, arXiv:1410.3012 [hep-ph].

[32] ATLAS Collaboration, ATLAS Pythia 8 tunes to 7 TeV data, ATL-PHYS-PUB-2014-021, https://cds.cern.ch/record/1966419, 2014.

[33] NNPDF Collaboration, R.D. Ball, et al., Parton distributions with LHC data, Nucl. Phys. B 867 (2013) 244, arXiv:1207.1303 [hep-ph].

[34] T. Sjöstrand, S. Mrenna, P. Skands, A brief introduction to PYTHIA 8.1, Comput. Phys. Commun. 178 (2008) 852, arXiv:0710.3820 [hep-ph].

[35] ATLAS Collaboration, The Pythia 8 A3 tune description of ATLAS minimum bias and inelastic measurements incorporating the Donnachie–Landshoff diffractive model, ATL-PHYS-PUB-2016-017, https://cds.cern.ch/record/2206965, 2016.

[36] J.A. Aguilar-Saavedra, Identifying top partners at LHC, J. High Energy Phys. 11 (2009) 030, arXiv:0907.3155 [hep-ph].

[37] M. Czakon, A. Mitov, Top++: a program for the calculation of the top-pair cross-section at hadron colliders, Comput. Phys. Commun. 185 (2014) 2930, arXiv:1112.5675 [hep-ph].

[38] S. Frixione, G. Ridolfi, P. Nason, A positive-weight next-to-leading-order Monte Carlo for heavy flavour hadroproduction, J. High Energy Phys. 09 (2007) 126, arXiv:0707.3088 [hep-ph].

[39] P. Nason, A new method for combining NLO QCD with shower Monte Carlo algorithms, J. High Energy Phys. 11 (2004) 040, arXiv:hep-ph/0409146.

[40] S. Frixione, P. Nason, C. Oleari, Matching NLO QCD computations with parton shower simulations: the POWHEG method, J. High Energy Phys. 11 (2007) 070, arXiv:0709.2092 [hep-ph].

[41] S. Alioli, P. Nason, C. Oleari, E. Re, A general framework for implementing NLO calculations in shower Monte Carlo programs: the POWHEG BOX, J. High Energy Phys. 06 (2010) 043, arXiv:1002.2581 [hep-ph].

[42] NNPDF Collaboration, R.D. Ball, et al., Parton distributions for the LHC run II, J. High Energy Phys. 04 (2015) 040, arXiv:1410.8849 [hep-ph].

[43] ATLAS Collaboration, Studies on top-quark Monte Carlo modelling for Top2016, ATL-PHYS-PUB-2016-020, https://cds.cern.ch/record/2216168, 2016.

[44] M. Bähr, et al., Herwig++ physics and manual, Eur. Phys. J. C 58 (2008) 639, arXiv:0803.0883 [hep-ph].

[45] J. Bellm, et al., Herwig 7.0/Herwig++ 3.0 release note, Eur. Phys. J. C 76 (2016) 196, arXiv:1512.01178 [hep-ph].

[46] L.A. Harland-Lang, A.D. Martin, P. Motylinski, R.S. Thorne, Parton distributions in the LHC era: MMHT 2014 PDFs, Eur. Phys. J. C 75 (2015) 204, arXiv:1412.3989 [hep-ph].

[47] J. Alwall, et al., The automated computation of tree-level and next-to-leading order differential cross sections, and their matching to parton shower simulations, J. High Energy Phys. 07 (2014) 079, arXiv:1405.0301 [hep-ph].

[48] ATLAS Collaboration, Study of top-quark pair modelling and uncertainties using ATLAS measurements at $\sqrt{s} = 13$ TeV, ATL-PHYS-PUB-2020-023, https://cds.cern.ch/record/2730443, 2020.

[49] S. Frixione, E. Laenen, P. Motylinski, C. White, B.R. Webber, Single-top hadroproduction in association with a W boson, J. High Energy Phys. 07 (2008) 029, arXiv:0805.3067 [hep-ph].

[50] R. Frederix, E. Re, P. Torrielli, Single-top t-channel hadroproduction in the four-flavour scheme with POWHEG and aMC@NLO, J. High Energy Phys. 09 (2012) 130, arXiv:1207.5391 [hep-ph].

[51] S. Alioli, P. Nason, C. Oleari, E. Re, NLO single-top production matched with shower in POWHEG: s- and t-channel contributions, J. High Energy Phys. 09 (2009) 111, arXiv:0907.4076 [hep-ph], Erratum: J. High Energy Phys. 02 (2010) 011.

[52] E. Bothmann, et al., Event generation with Sherpa 2.2, SciPost Phys. 7 (2019) 034, arXiv:1905.09127 [hep-ph].

[53] C. Anastasiou, L. Dixon, K. Melnikov, F. Petriello, High-precision QCD at hadron colliders: electroweak gauge boson rapidity distributions at next-to-next-to leading order, Phys. Rev. D 69 (2004) 094008, arXiv:hep-ph/0312266.

[54] T. Gleisberg, S. Höche, Comix, a new matrix element generator, J. High Energy Phys. 12 (2008) 039, arXiv:0808.3674 [hep-ph].

[55] S. Schumann, F. Krauss, A parton shower algorithm based on Catani–Seymour dipole factorisation, J. High Energy Phys. 03 (2008) 038, arXiv:0709.1027 [hep-ph].

[56] F. Buccioni, et al., OpenLoops 2, Eur. Phys. J. C 79 (2019) 866, arXiv:1907.13071 [hep-ph].

[57] F. Cascioli, P. Maierhöfer, S. Pozzorini, Scattering amplitudes with open loops, Phys. Rev. Lett. 108 (2012) 111601, arXiv:1111.5206 [hep-ph].

[58] A. Denner, S. Dittmaier, L. Hofer, Collier: a fortran-based complex one-loop library in extended regularizations, Comput. Phys. Commun. 212 (2017) 220, arXiv:1604.06792 [hep-ph].

[59] J. Gao, et al., CT10 next-to-next-to-leading order global analysis of QCD, Phys. Rev. D 89 (2014) 033009, arXiv:1302.6246 [hep-ph].

[60] D.J. Lange, The EvtGen particle decay simulation package, Nucl. Instrum. Methods A 462 (2001) 152.

[61] ATLAS Collaboration, Vertex reconstruction performance of the ATLAS detector at $\sqrt{s} = 13$ TeV, ATL-PHYS-PUB-2015-026, https://cds.cern.ch/record/2037717, 2015.

[62] ATLAS Collaboration, Electron and photon performance measurements with the ATLAS detector using the 2015–2017 LHC proton–proton collision data, J. Instrum. 14 (2019) P12006, arXiv:1908.00005 [hep-ex].

[63] ATLAS Collaboration, Muon reconstruction and identification efficiency in ATLAS using the full Run 2 pp collision data set at $\sqrt{s} = 13$ TeV, Eur. Phys. J. C 81 (2021) 578, arXiv:2012.00578 [hep-ex].

[64] ATLAS Collaboration, Studies of the muon momentum calibration and performance of the ATLAS detector with pp collisions at $\sqrt{s} = 13\,TeV$, Eur. Phys. J. C 83 (2023) 686, arXiv:2212.07338 [hep-ex].

[65] ATLAS Collaboration, Jet reconstruction and performance using particle flow with the ATLAS detector, Eur. Phys. J. C 77 (2017) 466, arXiv:1703.10485 [hep-ex].

[66] M. Cacciari, G.P. Salam, G. Soyez, The anti-k_t jet clustering algorithm, J. High Energy Phys. 04 (2008) 063, arXiv:0802.1189 [hep-ph].

[67] M. Cacciari, G.P. Salam, G. Soyez, FastJet user manual, Eur. Phys. J. C 72 (2012) 1896, arXiv:1111.6097 [hep-ph].

[68] ATLAS Collaboration, Jet energy scale and resolution measured in proton–proton collisions at $\sqrt{s} = 13\,TeV$ with the ATLAS detector, Eur. Phys. J. C 81 (2021) 689, arXiv:2007.02645 [hep-ex].

[69] ATLAS Collaboration, Performance of pile-up mitigation techniques for jets in pp collisions at $\sqrt{s} = 8\,TeV$ using the ATLAS detector, Eur. Phys. J. C 76 (2016) 581, arXiv:1510.03823 [hep-ex].

[70] ATLAS Collaboration, ATLAS flavour-tagging algorithms for the LHC Run 2 pp collision dataset, Eur. Phys. J. C 83 (2023) 681, arXiv:2211.16345 [physics.data-an].

[71] ATLAS Collaboration, ATLAS b-jet identification performance and efficiency measurement with $t\bar{t}$ events in pp collisions at $\sqrt{s} = 13\,TeV$, Eur. Phys. J. C 79 (2019) 970, arXiv:1907.05120 [hep-ex].

[72] ATLAS Collaboration, Calibration of the light-flavour jet mistagging efficiency of the b-tagging algorithms with Z+jets events using 139 fb^{-1} of ATLAS proton-proton collision data at $\sqrt{s} = 13$ TeV, Eur. Phys. J. C 83 (2023) 728, arXiv:2301.06319 [hep-ex].
[73] ATLAS Collaboration, Measurement of the c-jet mistagging efficiency in $t\bar{t}$ events using pp collision data at $\sqrt{s} = 13\,TeV$ collected with the ATLAS detector, Eur. Phys. J. C 82 (2022) 95, arXiv:2109.10627 [hep-ex].
[74] ATLAS Collaboration, Performance of missing transverse momentum reconstruction with the ATLAS detector using proton–proton collisions at $\sqrt{s} = 13\,TeV$, Eur. Phys. J. C 78 (2018) 903, arXiv:1802.08168 [hep-ex].
[75] ATLAS Collaboration, Topological cell clustering in the ATLAS calorimeters and its performance in LHC Run 1, Eur. Phys. J. C 77 (2017) 490, arXiv:1603.02934 [hep-ex].
[76] D. Krohn, J. Thaler, L.-T. Wang, Jet trimming, J. High Energy Phys. 02 (2010) 084, arXiv:0912.1342 [hep-ph].
[77] ATLAS Collaboration, In situ calibration of large-radius jet energy and mass in 13 TeV proton–proton collisions with the ATLAS detector, Eur. Phys. J. C 79 (2019) 135, arXiv:1807.09477 [hep-ex].
[78] ATLAS Collaboration, Measurement of the ATLAS detector jet mass response using forward folding with 80 fb^{-1} of $\sqrt{s} = 13$ TeV pp data, ATLAS-CONF-2020-022, https://cds.cern.ch/record/2724442, 2020.
[79] ATLAS Collaboration, Performance of top-quark and W-boson tagging with ATLAS in Run 2 of the LHC, Eur. Phys. J. C 79 (2019) 375, arXiv:1808.07858 [hep-ex].
[80] A.J. Larkoski, I. Moult, D. Neill, Power counting to better jet observables, J. High Energy Phys. 12 (2014) 009, arXiv:1409.6298 [hep-ph].
[81] ATLAS Collaboration, Boosted hadronic vector boson and top quark tagging with ATLAS using Run 2 data, ATL-PHYS-PUB-2020-017, https://cds.cern.ch/record/2724149, 2020.
[82] ATLAS Collaboration, ATLAS simulation of boson plus jets processes in Run 2, ATL-PHYS-PUB-2017-006, https://cds.cern.ch/record/2261937, 2017.
[83] A.D. Martin, W.J. Stirling, R.S. Thorne, G. Watt, Parton distributions for the LHC, Eur. Phys. J. C 63 (2009) 189, arXiv:0901.0002 [hep-ph].
[84] ATLAS Collaboration, Measurements of top-quark pair differential cross-sections in the $e\mu$ channel in pp collisions at $\sqrt{s} = 13\,TeV$ using the ATLAS detector, Eur. Phys. J. C 77 (2017) 292, arXiv:1612.05220 [hep-ex].
[85] ATLAS Collaboration, Tools for estimating fake/non-prompt lepton backgrounds with the ATLAS detector at the LHC, J. Instrum. 18 (2023) T11004, arXiv:2211.16178 [hep-ex].
[86] ATLAS Collaboration, Estimation of non-prompt and fake lepton backgrounds in final states with top quarks produced in proton-proton collisions at $\sqrt{s} = 8$ TeV with the ATLAS detector, ATLAS-CONF-2014-058, https://cds.cern.ch/record/1951336, 2014.
[87] ATLAS Collaboration, Studies of $t\bar{t}/tW$ interference effects in $b\bar{b}\ell^+\ell^{-\prime}\nu\bar{\nu}'$ final states with Powheg and MadGraph5_aMC@NLO setups, ATL-PHYS-PUB-2021-042, https://cds.cern.ch/record/2792254, 2021.
[88] J. Butterworth, et al., PDF4LHC recommendations for LHC Run II, J. Phys. G 43 (2016) 023001, arXiv:1510.03865 [hep-ph].
[89] A.L. Read, Presentation of search results: the CL_s technique, J. Phys. G 28 (2002) 2693.
[90] T. Junk, Confidence level computation for combining searches with small statistics, Nucl. Instrum. Methods A 434 (1999) 435, arXiv:hep-ex/9902006.
[91] G. Cowan, K. Cranmer, E. Gross, O. Vitells, Asymptotic formulae for likelihood-based tests of new physics, Eur. Phys. J. C 71 (2011) 1554, arXiv:1007.1727 [physics.data-an], Erratum: Eur. Phys. J. C 73 (2013) 2501.
[92] ATLAS Collaboration, ATLAS computing acknowledgements, ATL-SOFT-PUB-2023-001, https://cds.cern.ch/record/2869272, 2023.

The ATLAS Collaboration

G. Aad [102], B. Abbott [120], K. Abeling [55], N.J. Abicht [49], S.H. Abidi [29], A. Aboulhorma [35e], H. Abramowicz [151], H. Abreu [150], Y. Abulaiti [117], B.S. Acharya [69a,69b,m], C. Adam Bourdarios [4], L. Adamczyk [86a], S.V. Addepalli [26], M.J. Addison [101], J. Adelman [115], A. Adiguzel [21c], T. Adye [134], A.A. Affolder [136], Y. Afik [39], M.N. Agaras [13], J. Agarwala [73a,73b], A. Aggarwal [100], C. Agheorghiesei [27c], A. Ahmad [36], F. Ahmadov [38,z], W.S. Ahmed [104], S. Ahuja [95], X. Ai [62e], G. Aielli [76a,76b], A. Aikot [163], M. Ait Tamlihat [35e], B. Aitbenchikh [35a], I. Aizenberg [169], M. Akbiyik [100], T.P.A. Åkesson [98], A.V. Akimov [37], D. Akiyama [168], N.N. Akolkar [24], S. Aktas [21a], K. Al Khoury [41], G.L. Alberghi [23b], J. Albert [165], P. Albicocco [53], G.L. Albouy [60], S. Alderweireldt [52], Z.L. Alegria [121], M. Aleksa [36], I.N. Aleksandrov [38], C. Alexa [27b], T. Alexopoulos [10], F. Alfonsi [23b], M. Algren [56], M. Alhroob [120], B. Ali [132], H.M.J. Ali [91], S. Ali [148], S.W. Alibocus [92], M. Aliev [33c], G. Alimonti [71a], W. Alkakhi [55], C. Allaire [66], B.M.M. Allbrooke [146], J.F. Allen [52], C.A. Allendes Flores [137f], P.P. Allport [20], A. Aloisio [72a,72b], F. Alonso [90], C. Alpigiani [138], M. Alvarez Estevez [99], A. Alvarez Fernandez [100], M. Alves Cardoso [56], M.G. Alviggi [72a,72b], M. Aly [101], Y. Amaral Coutinho [83b], A. Ambler [104], C. Amelung [36], M. Amerl [101], C.G. Ames [109], D. Amidei [106], S.P. Amor Dos Santos [130a], K.R. Amos [163], V. Ananiev [125], C. Anastopoulos [139], T. Andeen [11], J.K. Anders [36], S.Y. Andrean [47a,47b], A. Andreazza [71a,71b], S. Angelidakis [9], A. Angerami [41,ac], A.V. Anisenkov [37], A. Annovi [74a], C. Antel [56], M.T. Anthony [139], E. Antipov [145], M. Antonelli [53], F. Anulli [75a], M. Aoki [84], T. Aoki [153], J.A. Aparisi Pozo [163], M.A. Aparo [146], L. Aperio Bella [48], C. Appelt [18], A. Apyan [26], S.J. Arbiol Val [87], C. Arcangeletti [53], A.T.H. Arce [51], E. Arena [92], J-F. Arguin [108], S. Argyropoulos [54], J.-H. Arling [48], O. Arnaez [4], H. Arnold [114], G. Artoni [75a,75b], H. Asada [111], K. Asai [118], S. Asai [153], N.A. Asbah [61], K. Assamagan [29], R. Astalos [28a], S. Atashi [159], R.J. Atkin [33a], M. Atkinson [162], H. Atmani [35f], P.A. Atmasiddha [128], K. Augsten [132], S. Auricchio [72a,72b], A.D. Auriol [20], V.A. Austrup [101], G. Avolio [36], K. Axiotis [56], G. Azuelos [108,ag], D. Babal [28b], H. Bachacou [135], K. Bachas [152,q], A. Bachiu [34], F. Backman [47a,47b], A. Badea [39], T.M. Baer [106], P. Bagnaia [75a,75b], M. Bahmani [18], D. Bahner [54], A.J. Bailey [163], V.R. Bailey [162], J.T. Baines [134], L. Baines [94], O.K. Baker [172], E. Bakos [15], D. Bakshi Gupta [8], V. Balakrishnan [120],

R. Balasubramanian [114], E.M. Baldin [37], P. Balek [86a], E. Ballabene [23b,23a], F. Balli [135], L.M. Baltes [63a], W.K. Balunas [32], J. Balz [100], E. Banas [87], M. Bandieramonte [129], A. Bandyopadhyay [24], S. Bansal [24], L. Barak [151], M. Barakat [48], E.L. Barberio [105], D. Barberis [57b,57a], M. Barbero [102], M.Z. Barel [114], K.N. Barends [33a], T. Barillari [110], M-S. Barisits [36], T. Barklow [143], P. Baron [122], D.A. Baron Moreno [101], A. Baroncelli [62a], G. Barone [29], A.J. Barr [126], J.D. Barr [96], F. Barreiro [99], J. Barreiro Guimarães da Costa [14a], U. Barron [151], M.G. Barros Teixeira [130a], S. Barsov [37], F. Bartels [63a], R. Bartoldus [143], A.E. Barton [91], P. Bartos [28a], A. Basan [100], M. Baselga [49], A. Bassalat [66,b], M.J. Basso [156a], C.R. Basson [101], R.L. Bates [59], S. Batlamous [35e], J.R. Batley [32], B. Batool [141], M. Battaglia [136], D. Battulga [18], M. Bauce [75a,75b], M. Bauer [36], P. Bauer [24], L.T. Bazzano Hurrell [30], J.B. Beacham [51], T. Beau [127], J.Y. Beaucamp [90], P.H. Beauchemin [158], P. Bechtle [24], H.P. Beck [19,p], K. Becker [167], A.J. Beddall [82], V.A. Bednyakov [38], C.P. Bee [145], L.J. Beemster [15], T.A. Beermann [36], M. Begalli [83d], M. Begel [29], A. Behera [145], J.K. Behr [48], J.F. Beirer [36], F. Beisiegel [24], M. Belfkir [116b], G. Bella [151], L. Bellagamba [23b], A. Bellerive [34], P. Bellos [20], K. Beloborodov [37], D. Benchekroun [35a], F. Bendebba [35a], Y. Benhammou [151], S. Bentvelsen [114], L. Beresford [48], M. Beretta [53], E. Bergeaas Kuutmann [161], N. Berger [4], B. Bergmann [132], J. Beringer [17a], G. Bernardi [5], C. Bernius [143], F.U. Bernlochner [24], F. Bernon [36,102], A. Berrocal Guardia [13], T. Berry [95], P. Berta [133], A. Berthold [50], I.A. Bertram [91], S. Bethke [110], A. Betti [75a,75b], A.J. Bevan [94], N.K. Bhalla [54], M. Bhamjee [33c], S. Bhatta [145], D.S. Bhattacharya [166], P. Bhattarai [143], K.D. Bhide [54], V.S. Bhopatkar [121], R.M. Bianchi [129], G. Bianco [23b,23a], O. Biebel [109], R. Bielski [123], M. Biglietti [77a], M. Bindi [55], A. Bingul [21b], C. Bini [75a,75b], A. Biondini [92], C.J. Birch-sykes [101], G.A. Bird [32,134], M. Birman [169], M. Biros [133], S. Biryukov [146], T. Bisanz [49], E. Bisceglie [43b,43a], J.P. Biswal [134], D. Biswas [141], K. Bjørke [125], I. Bloch [48], A. Blue [59], U. Blumenschein [94], J. Blumenthal [100], G.J. Bobbink [114], V.S. Bobrovnikov [37], M. Boehler [54], B. Boehm [166], D. Bogavac [36], A.G. Bogdanchikov [37], C. Bohm [47a], V. Boisvert [95], P. Bokan [36], T. Bold [86a], M. Bomben [5], M. Bona [94], M. Boonekamp [135], C.D. Booth [95], A.G. Borbély [59], I.S. Bordulev [37], H.M. Borecka-Bielska [108], G. Borissov [91], D. Bortoletto [126], D. Boscherini [23b], M. Bosman [13], J.D. Bossio Sola [36], K. Bouaouda [35a], N. Bouchhar [163], J. Boudreau [129], E.V. Bouhova-Thacker [91], D. Boumediene [40], R. Bouquet [165], A. Boveia [119], J. Boyd [36], D. Boye [29], I.R. Boyko [38], J. Bracinik [20], N. Brahimi [62d], G. Brandt [171], O. Brandt [32], F. Braren [48], B. Brau [103], J.E. Brau [123], R. Brener [169], L. Brenner [114], R. Brenner [161], S. Bressler [169], D. Britton [59], D. Britzger [110], I. Brock [24], G. Brooijmans [41], W.K. Brooks [137f], E. Brost [29], L.M. Brown [165], L.E. Bruce [61], T.L. Bruckler [126], P.A. Bruckman de Renstrom [87], B. Brüers [48], A. Bruni [23b], G. Bruni [23b], M. Bruschi [23b], N. Bruscino [75a,75b], T. Buanes [16], Q. Buat [138], D. Buchin [110], A.G. Buckley [59], O. Bulekov [37], B.A. Bullard [143], S. Burdin [92], C.D. Burgard [49], A.M. Burger [40], B. Burghgrave [8], O. Burlayenko [54], J.T.P. Burr [32], C.D. Burton [11], J.C. Burzynski [142], E.L. Busch [41], V. Büscher [100], P.J. Bussey [59], J.M. Butler [25], C.M. Buttar [59], J.M. Butterworth [96], W. Buttinger [134], C.J. Buxo Vazquez [107], A.R. Buzykaev [37], S. Cabrera Urbán [163], L. Cadamuro [66], D. Caforio [58], H. Cai [129], Y. Cai [14a,14e], Y. Cai [14c], V.M.M. Cairo [36], O. Cakir [3a], N. Calace [36], P. Calafiura [17a], G. Calderini [127], P. Calfayan [68], G. Callea [59], L.P. Caloba [83b], D. Calvet [40], S. Calvet [40], M. Calvetti [74a,74b], R. Camacho Toro [127], S. Camarda [36], D. Camarero Munoz [26], P. Camarri [76a,76b], M.T. Camerlingo [72a,72b], D. Cameron [36], C. Camincher [165], M. Campanelli [96], A. Camplani [42], V. Canale [72a,72b], J. Cantero [163], Y. Cao [162], F. Capocasa [26], M. Capua [43b,43a], A. Carbone [71a,71b], R. Cardarelli [76a], J.C.J. Cardenas [8], F. Cardillo [163], G. Carducci [43b,43a], T. Carli [36], G. Carlino [72a],

J.I. Carlotto [13], B.T. Carlson [129,r], E.M. Carlson [165,156a], L. Carminati [71a,71b], A. Carnelli [135], M. Carnesale [75a,75b], S. Caron [113], E. Carquin [137f], S. Carrá [71a], G. Carratta [23b,23a], A.M. Carroll [123], J.W.S. Carter [155], T.M. Carter [52], M.P. Casado [13,i], M. Caspar [48], F.L. Castillo [4], L. Castillo Garcia [13], V. Castillo Gimenez [163], N.F. Castro [130a,130e], A. Catinaccio [36], J.R. Catmore [125], T. Cavaliere [4], V. Cavaliere [29], N. Cavalli [23b,23a], V. Cavasinni [74a,74b], Y.C. Cekmecelioglu [48], E. Celebi [21a], F. Celli [126], M.S. Centonze [70a,70b], V. Cepaitis [56], K. Cerny [122], A.S. Cerqueira [83a], A. Cerri [146], L. Cerrito [76a,76b], F. Cerutti [17a], B. Cervato [141], A. Cervelli [23b], G. Cesarini [53], S.A. Cetin [82], D. Chakraborty [115], J. Chan [17a], W.Y. Chan [153], J.D. Chapman [32], E. Chapon [135], B. Chargeishvili [149b], D.G. Charlton [20], M. Chatterjee [19], C. Chauhan [133], Y. Che [14c], S. Chekanov [6], S.V. Chekulaev [156a], G.A. Chelkov [38,a], A. Chen [106], B. Chen [151], B. Chen [165], H. Chen [14c], H. Chen [29], J. Chen [62c], J. Chen [142], M. Chen [126], S. Chen [153], S.J. Chen [14c], X. Chen [62c,135], X. Chen [14b,af], Y. Chen [62a], C.L. Cheng [170], H.C. Cheng [64a], S. Cheong [143], A. Cheplakov [38], E. Cheremushkina [48], E. Cherepanova [114], R. Cherkaoui El Moursli [35e], E. Cheu [7], K. Cheung [65], L. Chevalier [135], V. Chiarella [53], G. Chiarelli [74a], N. Chiedde [102], G. Chiodini [70a], A.S. Chisholm [20], A. Chitan [27b], M. Chitishvili [163], M.V. Chizhov [38,a], K. Choi [11], Y. Chou [138], E.Y.S. Chow [113], K.L. Chu [169], M.C. Chu [64a], X. Chu [14a,14e], J. Chudoba [131], J.J. Chwastowski [87], D. Cieri [110], K.M. Ciesla [86a], V. Cindro [93], A. Ciocio [17a], F. Cirotto [72a,72b], Z.H. Citron [169,k], M. Citterio [71a], D.A. Ciubotaru [27b], A. Clark [56], P.J. Clark [52], C. Clarry [155], J.M. Clavijo Columbie [48], S.E. Clawson [48], C. Clement [47a,47b], J. Clercx [48], Y. Coadou [102], M. Cobal [69a,69c], A. Coccaro [57b], R.F. Coelho Barrue [130a], R. Coelho Lopes De Sa [103], S. Coelli [71a], B. Cole [41], J. Collot [60], P. Conde Muiño [130a,130g], M.P. Connell [33c], S.H. Connell [33c], I.A. Connelly [59], E.I. Conroy [126], F. Conventi [72a,ah], H.G. Cooke [20], A.M. Cooper-Sarkar [126], A. Cordeiro Oudot Choi [127], L.D. Corpe [40], M. Corradi [75a,75b], F. Corriveau [104,x], A. Cortes-Gonzalez [18], M.J. Costa [163], F. Costanza [4], D. Costanzo [139], B.M. Cote [119], G. Cowan [95], K. Cranmer [170], D. Cremonini [23b,23a], S. Crépé-Renaudin [60], F. Crescioli [127], M. Cristinziani [141], M. Cristoforetti [78a,78b], V. Croft [114], J.E. Crosby [121], G. Crosetti [43b,43a], A. Cueto [99], T. Cuhadar Donszelmann [159], H. Cui [14a,14e], Z. Cui [7], W.R. Cunningham [59], F. Curcio [43b,43a], P. Czodrowski [36], M.M. Czurylo [63b], M.J. Da Cunha Sargedas De Sousa [57b,57a], J.V. Da Fonseca Pinto [83b], C. Da Via [101], W. Dabrowski [86a], T. Dado [49], S. Dahbi [33g], T. Dai [106], D. Dal Santo [19], C. Dallapiccola [103], M. Dam [42], G. D'amen [29], V. D'Amico [109], J. Damp [100], J.R. Dandoy [34], M. Danninger [142], V. Dao [36], G. Darbo [57b], S. Darmora [6], S.J. Das [29,aj], S. D'Auria [71a,71b], C. David [33a], T. Davidek [133], B. Davis-Purcell [34], I. Dawson [94], H.A. Day-hall [132], K. De [8], R. De Asmundis [72a], N. De Biase [48], S. De Castro [23b,23a], N. De Groot [113], P. de Jong [114], H. De la Torre [115], A. De Maria [14c], A. De Salvo [75a], U. De Sanctis [76a,76b], F. De Santis [70a,70b], A. De Santo [146], J.B. De Vivie De Regie [60], D.V. Dedovich [38], J. Degens [114], A.M. Deiana [44], F. Del Corso [23b,23a], J. Del Peso [99], F. Del Rio [63a], L. Delagrange [127], F. Deliot [135], C.M. Delitzsch [49], M. Della Pietra [72a,72b], D. Della Volpe [56], A. Dell'Acqua [36], L. Dell'Asta [71a,71b], M. Delmastro [4], P.A. Delsart [60], S. Demers [172], M. Demichev [38], S.P. Denisov [37], L. D'Eramo [40], D. Derendarz [87], F. Derue [127], P. Dervan [92], K. Desch [24], C. Deutsch [24], F.A. Di Bello [57b,57a], A. Di Ciaccio [76a,76b], L. Di Ciaccio [4], A. Di Domenico [75a,75b], C. Di Donato [72a,72b], A. Di Girolamo [36], G. Di Gregorio [36], A. Di Luca [78a,78b], B. Di Micco [77a,77b], R. Di Nardo [77a,77b], M. Diamantopoulou [34], F.A. Dias [114], T. Dias Do Vale [142], M.A. Diaz [137a,137b], F.G. Diaz Capriles [24], M. Didenko [163], E.B. Diehl [106], L. Diehl [54], S. Díez Cornell [48], C. Diez Pardos [141], C. Dimitriadi [161,24], A. Dimitrievska [17a], J. Dingfelder [24], I-M. Dinu [27b], S.J. Dittmeier [63b], F. Dittus [36], F. Djama [102],

T. Djobava [149b], C. Doglioni [101,98], A. Dohnalova [28a], J. Dolejsi [133], Z. Dolezal [133], K.M. Dona [39], M. Donadelli [83c], B. Dong [107], J. Donini [40], A. D'Onofrio [72a,72b], M. D'Onofrio [92], J. Dopke [134], A. Doria [72a], N. Dos Santos Fernandes [130a], P. Dougan [101], M.T. Dova [90], A.T. Doyle [59], M.A. Draguet [126], E. Dreyer [169], I. Drivas-koulouris [10], M. Drnevich [117], M. Drozdova [56], D. Du [62a], T.A. du Pree [114], F. Dubinin [37], M. Dubovsky [28a], E. Duchovni [169], G. Duckeck [109], O.A. Ducu [27b], D. Duda [52], A. Dudarev [36], E.R. Duden [26], M. D'uffizi [101], L. Duflot [66], M. Dührssen [36], A.E. Dumitriu [27b], M. Dunford [63a], S. Dungs [49], K. Dunne [47a,47b], A. Duperrin [102], H. Duran Yildiz [3a], M. Düren [58], A. Durglishvili [149b], B.L. Dwyer [115], G.I. Dyckes [17a], M. Dyndal [86a], B.S. Dziedzic [87], Z.O. Earnshaw [146], G.H. Eberwein [126], B. Eckerova [28a], S. Eggebrecht [55], E. Egidio Purcino De Souza [127], L.F. Ehrke [56], G. Eigen [16], K. Einsweiler [17a], T. Ekelof [161], P.A. Ekman [98], S. El Farkh [35b], Y. El Ghazali [35b], H. El Jarrari [36], A. El Moussaouy [108], V. Ellajosyula [161], M. Ellert [161], F. Ellinghaus [171], N. Ellis [36], J. Elmsheuser [29], M. Elsing [36], D. Emeliyanov [134], Y. Enari [153], I. Ene [17a], S. Epari [13], P.A. Erland [87], M. Errenst [171], M. Escalier [66], C. Escobar [163], E. Etzion [151], G. Evans [130a], H. Evans [68], L.S. Evans [95], M.O. Evans [146], A. Ezhilov [37], S. Ezzarqtouni [35a], F. Fabbri [59], L. Fabbri [23b,23a], G. Facini [96], V. Fadeyev [136], R.M. Fakhrutdinov [37], D. Fakoudis [100], S. Falciano [75a], L.F. Falda Ulhoa Coelho [36], P.J. Falke [24], J. Faltova [133], C. Fan [162], Y. Fan [14a], Y. Fang [14a,14e], M. Fanti [71a,71b], M. Faraj [69a,69b], Z. Farazpay [97], A. Farbin [8], A. Farilla [77a], T. Farooque [107], S.M. Farrington [52], F. Fassi [35e], D. Fassouliotis [9], M. Faucci Giannelli [76a,76b], W.J. Fawcett [32], L. Fayard [66], P. Federic [133], P. Federicova [131], O.L. Fedin [37,a], G. Fedotov [37], M. Feickert [170], L. Feligioni [102], D.E. Fellers [123], C. Feng [62b], M. Feng [14b], Z. Feng [114], M.J. Fenton [159], A.B. Fenyuk [37], L. Ferencz [48], R.A.M. Ferguson [91], S.I. Fernandez Luengo [137f], P. Fernandez Martinez [13], M.J.V. Fernoux [102], J. Ferrando [91], A. Ferrari [161], P. Ferrari [114,113], R. Ferrari [73a], D. Ferrere [56], C. Ferretti [106], F. Fiedler [100], P. Fiedler [132], A. Filipčič [93], E.K. Filmer [1], F. Filthaut [113], M.C.N. Fiolhais [130a,130c,c], L. Fiorini [163], W.C. Fisher [107], T. Fitschen [101], P.M. Fitzhugh [135], I. Fleck [141], P. Fleischmann [106], T. Flick [171], M. Flores [33d,ad], L.R. Flores Castillo [64a], L. Flores Sanz De Acedo [36], F.M. Follega [78a,78b], N. Fomin [16], J.H. Foo [155], A. Formica [135], A.C. Forti [101], E. Fortin [36], A.W. Fortman [17a], M.G. Foti [17a], L. Fountas [9,j], D. Fournier [66], H. Fox [91], P. Francavilla [74a,74b], S. Francescato [61], S. Franchellucci [56], M. Franchini [23b,23a], S. Franchino [63a], D. Francis [36], L. Franco [113], V. Franco Lima [36], L. Franconi [48], M. Franklin [61], G. Frattari [26], A.C. Freegard [94], W.S. Freund [83b], Y.Y. Frid [151], J. Friend [59], N. Fritzsche [50], A. Froch [54], D. Froidevaux [36], J.A. Frost [126], Y. Fu [62a], S. Fuenzalida Garrido [137f], M. Fujimoto [102], K.Y. Fung [64a], E. Furtado De Simas Filho [83b], M. Furukawa [153], J. Fuster [163], A. Gabrielli [23b,23a], A. Gabrielli [155], P. Gadow [36], G. Gagliardi [57b,57a], L.G. Gagnon [17a], E.J. Gallas [126], B.J. Gallop [134], K.K. Gan [119], S. Ganguly [153], Y. Gao [52], F.M. Garay Walls [137a,137b], B. Garcia [29], C. García [163], A. Garcia Alonso [114], A.G. Garcia Caffaro [172], J.E. García Navarro [163], M. Garcia-Sciveres [17a], G.L. Gardner [128], R.W. Gardner [39], N. Garelli [158], D. Garg [80], R.B. Garg [143,n], J.M. Gargan [52], C.A. Garner [155], C.M. Garvey [33a], P. Gaspar [83b], V.K. Gassmann [158], G. Gaudio [73a], V. Gautam [13], P. Gauzzi [75a,75b], I.L. Gavrilenko [37], A. Gavrilyuk [37], C. Gay [164], G. Gaycken [48], E.N. Gazis [10], A.A. Geanta [27b], C.M. Gee [136], A. Gekow [119], C. Gemme [57b], M.H. Genest [60], S. Gentile [75a,75b], A.D. Gentry [112], S. George [95], W.F. George [20], T. Geralis [46], P. Gessinger-Befurt [36], M.E. Geyik [171], M. Ghani [167], M. Ghneimat [141], K. Ghorbanian [94], A. Ghosal [141], A. Ghosh [159], A. Ghosh [7], B. Giacobbe [23b], S. Giagu [75a,75b], T. Giani [114],

P. Giannetti [74a], A. Giannini [62a], S.M. Gibson [95], M. Gignac [136], D.T. Gil [86b], A.K. Gilbert [86a], B.J. Gilbert [41], D. Gillberg [34], G. Gilles [114], L. Ginabat [127], D.M. Gingrich [2,ag], M.P. Giordani [69a,69c], P.F. Giraud [135], G. Giugliarelli [69a,69c], D. Giugni [71a], F. Giuli [36], I. Gkialas [9,j], L.K. Gladilin [37], C. Glasman [99], G.R. Gledhill [123], G. Glemža [48], M. Glisic [123], I. Gnesi [43b,f], Y. Go [29], M. Goblirsch-Kolb [36], B. Gocke [49], D. Godin [108], B. Gokturk [21a], S. Goldfarb [105], T. Golling [56], M.G.D. Gololo [33g], D. Golubkov [37], J.P. Gombas [107], A. Gomes [130a,130b], G. Gomes Da Silva [141], A.J. Gomez Delegido [163], R. Gonçalo [130a,130c], L. Gonella [20], A. Gongadze [149c], F. Gonnella [20], J.L. Gonski [41], R.Y. González Andana [52], S. González de la Hoz [163], R. Gonzalez Lopez [92], C. Gonzalez Renteria [17a], M.V. Gonzalez Rodrigues [48], R. Gonzalez Suarez [161], S. Gonzalez-Sevilla [56], G.R. Gonzalvo Rodriguez [163], L. Goossens [36], B. Gorini [36], E. Gorini [70a,70b], A. Gorišek [93], T.C. Gosart [128], A.T. Goshaw [51], M.I. Gostkin [38], S. Goswami [121], C.A. Gottardo [36], S.A. Gotz [109], M. Gouighri [35b], V. Goumarre [48], A.G. Goussiou [138], N. Govender [33c], I. Grabowska-Bold [86a], K. Graham [34], E. Gramstad [125], S. Grancagnolo [70a,70b], M. Grandi [146], C.M. Grant [1,135], P.M. Gravila [27f], F.G. Gravili [70a,70b], H.M. Gray [17a], M. Greco [70a,70b], C. Grefe [24], I.M. Gregor [48], P. Grenier [143], S.G. Grewe [110], C. Grieco [13], A.A. Grillo [136], K. Grimm [31], S. Grinstein [13,t], J.-F. Grivaz [66], E. Gross [169], J. Grosse-Knetter [55], J.C. Grundy [126], L. Guan [106], W. Guan [29], C. Gubbels [164], J.G.R. Guerrero Rojas [163], G. Guerrieri [69a,69c], F. Guescini [110], R. Gugel [100], J.A.M. Guhit [106], A. Guida [18], E. Guilloton [167,134], S. Guindon [36], F. Guo [14a,14e], J. Guo [62c], L. Guo [48], Y. Guo [106], R. Gupta [48], R. Gupta [129], S. Gurbuz [24], S.S. Gurdasani [54], G. Gustavino [36], M. Guth [56], P. Gutierrez [120], L.F. Gutierrez Zagazeta [128], M. Gutsche [50], C. Gutschow [96], C. Gwenlan [126], C.B. Gwilliam [92], E.S. Haaland [125], A. Haas [117], M. Habedank [48], C. Haber [17a], H.K. Hadavand [8], A. Hadef [50], S. Hadzic [110], A.I. Hagan [91], J.J. Hahn [141], E.H. Haines [96], M. Haleem [166], J. Haley [121], J.J. Hall [139], G.D. Hallewell [102], L. Halser [19], K. Hamano [165], M. Hamer [24], G.N. Hamity [52], E.J. Hampshire [95], J. Han [62b], K. Han [62a], L. Han [14c], L. Han [62a], S. Han [17a], Y.F. Han [155], K. Hanagaki [84], M. Hance [136], D.A. Hangal [41], H. Hanif [142], M.D. Hank [128], J.B. Hansen [42], P.H. Hansen [42], K. Hara [157], D. Harada [56], T. Harenberg [171], S. Harkusha [37], M.L. Harris [103], Y.T. Harris [126], J. Harrison [13], N.M. Harrison [119], P.F. Harrison [167], N.M. Hartman [110], N.M. Hartmann [109], Y. Hasegawa [140], R. Hauser [107], C.M. Hawkes [20], R.J. Hawkings [36], Y. Hayashi [153], S. Hayashida [111], D. Hayden [107], C. Hayes [106], R.L. Hayes [114], C.P. Hays [126], J.M. Hays [94], H.S. Hayward [92], F. He [62a], M. He [14a,14e], Y. He [154], Y. He [48], N.B. Heatley [94], V. Hedberg [98], A.L. Heggelund [125], N.D. Hehir [94,*], C. Heidegger [54], K.K. Heidegger [54], W.D. Heidorn [81], J. Heilman [34], S. Heim [48], T. Heim [17a], J.G. Heinlein [128], J.J. Heinrich [123], L. Heinrich [110,ae], J. Hejbal [131], A. Held [170], S. Hellesund [16], C.M. Helling [164], S. Hellman [47a,47b], R.C.W. Henderson [91], L. Henkelmann [32], A.M. Henriques Correia [36], H. Herde [98], Y. Hernández Jiménez [145], L.M. Herrmann [24], T. Herrmann [50], G. Herten [54], R. Hertenberger [109], L. Hervas [36], M.E. Hesping [100], N.P. Hessey [156a], E. Hill [155], S.J. Hillier [20], J.R. Hinds [107], F. Hinterkeuser [24], M. Hirose [124], S. Hirose [157], D. Hirschbuehl [171], T.G. Hitchings [101], B. Hiti [93], J. Hobbs [145], R. Hobincu [27e], N. Hod [169], M.C. Hodgkinson [139], B.H. Hodkinson [32], A. Hoecker [36], D.D. Hofer [106], J. Hofer [48], T. Holm [24], M. Holzbock [110], L.B.A.H. Hommels [32], B.P. Honan [101], J. Hong [62c], T.M. Hong [129], B.H. Hooberman [162], W.H. Hopkins [6], Y. Horii [111], S. Hou [148], A.S. Howard [93], J. Howarth [59], J. Hoya [6], M. Hrabovsky [122], A. Hrynevich [48], T. Hryn'ova [4], P.J. Hsu [65], S.-C. Hsu [138], Q. Hu [62a], Y.F. Hu [14a,14e], S. Huang [64b], X. Huang [14c], X. Huang [14a,14e],

Y. Huang [139], Y. Huang [14a], Z. Huang [101], Z. Hubacek [132], M. Huebner [24], F. Huegging [24], T.B. Huffman [126], C.A. Hugli [48], M. Huhtinen [36], S.K. Huiberts [16], R. Hulsken [104], N. Huseynov [12], J. Huston [107], J. Huth [61], R. Hyneman [143], G. Iacobucci [56], G. Iakovidis [29], I. Ibragimov [141], L. Iconomidou-Fayard [66], J.P. Iddon [36], P. Iengo [72a,72b], R. Iguchi [153], T. Iizawa [126], Y. Ikegami [84], N. Ilic [155], H. Imam [35a], M. Ince Lezki [56], T. Ingebretsen Carlson [47a,47b], G. Introzzi [73a,73b], M. Iodice [77a], V. Ippolito [75a,75b], R.K. Irwin [92], M. Ishino [153], W. Islam [170], C. Issever [18,48], S. Istin [21a,al], H. Ito [168], J.M. Iturbe Ponce [64a], R. Iuppa [78a,78b], A. Ivina [169], J.M. Izen [45], V. Izzo [72a], P. Jacka [131,132], P. Jackson [1], B.P. Jaeger [142], C.S. Jagfeld [109], G. Jain [156a], P. Jain [54], K. Jakobs [54], T. Jakoubek [169], J. Jamieson [59], K.W. Janas [86a], M. Javurkova [103], L. Jeanty [123], J. Jejelava [149a,aa], P. Jenni [54,g], C.E. Jessiman [34], C. Jia [62b], J. Jia [145], X. Jia [61], X. Jia [14a,14e], Z. Jia [14c], S. Jiggins [48], J. Jimenez Pena [13], S. Jin [14c], A. Jinaru [27b], O. Jinnouchi [154], P. Johansson [139], K.A. Johns [7], J.W. Johnson [136], D.M. Jones [32], E. Jones [48], P. Jones [32], R.W.L. Jones [91], T.J. Jones [92], H.L. Joos [55,36], R. Joshi [119], J. Jovicevic [15], X. Ju [17a], J.J. Junggeburth [103], T. Junkermann [63a], A. Juste Rozas [13,t], M.K. Juzek [87], S. Kabana [137e], A. Kaczmarska [87], M. Kado [110], H. Kagan [119], M. Kagan [143], A. Kahn [41], A. Kahn [128], C. Kahra [100], T. Kaji [153], E. Kajomovitz [150], N. Kakati [169], I. Kalaitzidou [54], C.W. Kalderon [29], A. Kamenshchikov [155], N.J. Kang [136], D. Kar [33g], K. Karava [126], M.J. Kareem [156b], E. Karentzos [54], I. Karkanias [152], O. Karkout [114], S.N. Karpov [38], Z.M. Karpova [38], V. Kartvelishvili [91], A.N. Karyukhin [37], E. Kasimi [152], J. Katzy [48], S. Kaur [34], K. Kawade [140], M.P. Kawale [120], C. Kawamoto [88], T. Kawamoto [62a], E.F. Kay [36], F.I. Kaya [158], S. Kazakos [107], V.F. Kazanin [37], Y. Ke [145], J.M. Keaveney [33a], R. Keeler [165], G.V. Kehris [61], J.S. Keller [34], A.S. Kelly [96], J.J. Kempster [146], P.D. Kennedy [100], O. Kepka [131], B.P. Kerridge [167], S. Kersten [171], B.P. Kerševan [93], S. Keshri [66], L. Keszeghova [28a], S. Ketabchi Haghighat [155], R.A. Khan [129], A. Khanov [121], A.G. Kharlamov [37], T. Kharlamova [37], E.E. Khoda [138], M. Kholodenko [37], T.J. Khoo [18], G. Khoriauli [166], J. Khubua [149b], Y.A.R. Khwaira [66], B. Kibirige [33g], A. Kilgallon [123], D.W. Kim [47a,47b], Y.K. Kim [39], N. Kimura [96], M.K. Kingston [55], A. Kirchhoff [55], C. Kirfel [24], F. Kirfel [24], J. Kirk [134], A.E. Kiryunin [110], C. Kitsaki [10], O. Kivernyk [24], M. Klassen [63a], C. Klein [34], L. Klein [166], M.H. Klein [44], S.B. Klein [56], U. Klein [92], P. Klimek [36], A. Klimentov [29], T. Klioutchnikova [36], P. Kluit [114], S. Kluth [110], E. Kneringer [79], T.M. Knight [155], A. Knue [49], R. Kobayashi [88], D. Kobylianskii [169], S.F. Koch [126], M. Kocian [143], P. Kodyš [133], D.M. Koeck [123], P.T. Koenig [24], T. Koffas [34], O. Kolay [50], I. Koletsou [4], T. Komarek [122], K. Köneke [54], A.X.Y. Kong [1], T. Kono [118], N. Konstantinidis [96], P. Kontaxakis [56], B. Konya [98], R. Kopeliansky [68], S. Koperny [86a], K. Korcyl [87], K. Kordas [152,e], A. Korn [96], S. Korn [55], I. Korolkov [13], N. Korotkova [37], B. Kortman [114], O. Kortner [110], S. Kortner [110], W.H. Kostecka [115], V.V. Kostyukhin [141], A. Kotsokechagia [135], A. Kotwal [51], A. Koulouris [36], A. Kourkoumeli-Charalampidi [73a,73b], C. Kourkoumelis [9], E. Kourlitis [110,ae], O. Kovanda [146], R. Kowalewski [165], W. Kozanecki [135], A.S. Kozhin [37], V.A. Kramarenko [37], G. Kramberger [93], P. Kramer [100], M.W. Krasny [127], A. Krasznahorkay [36], J.W. Kraus [171], J.A. Kremer [48], T. Kresse [50], J. Kretzschmar [92], K. Kreul [18], P. Krieger [155], S. Krishnamurthy [103], M. Krivos [133], K. Krizka [20], K. Kroeninger [49], H. Kroha [110], J. Kroll [131], J. Kroll [128], K.S. Krowpman [107], U. Kruchonak [38], H. Krüger [24], N. Krumnack [81], M.C. Kruse [51], O. Kuchinskaia [37], S. Kuday [3a], S. Kuehn [36], R. Kuesters [54], T. Kuhl [48], V. Kukhtin [38], Y. Kulchitsky [37,a], S. Kuleshov [137d,137b], M. Kumar [33g], N. Kumari [48], P. Kumari [156b], A. Kupco [131], T. Kupfer [49], A. Kupich [37], O. Kuprash [54],

H. Kurashige [85], L.L. Kurchaninov [156a], O. Kurdysh [66], Y.A. Kurochkin [37], A. Kurova [37], M. Kuze [154], A.K. Kvam [103], J. Kvita [122], T. Kwan [104], N.G. Kyriacou [106], L.A.O. Laatu [102], C. Lacasta [163], F. Lacava [75a,75b], H. Lacker [18], D. Lacour [127], N.N. Lad [96], E. Ladygin [38], B. Laforge [127], T. Lagouri [27b], F.Z. Lahbabi [35a], S. Lai [55], I.K. Lakomiec [86a], N. Lalloue [60], J.E. Lambert [165], S. Lammers [68], W. Lampl [7], C. Lampoudis [152,e], A.N. Lancaster [115], E. Lançon [29], U. Landgraf [54], M.P.J. Landon [94], V.S. Lang [54], R.J. Langenberg [103], O.K.B. Langrekken [125], A.J. Lankford [159], F. Lanni [36], K. Lantzsch [24], A. Lanza [73a], A. Lapertosa [57b,57a], J.F. Laporte [135], T. Lari [71a], F. Lasagni Manghi [23b], M. Lassnig [36], V. Latonova [131], A. Laudrain [100], A. Laurier [150], S.D. Lawlor [139], Z. Lawrence [101], R. Lazaridou [167], M. Lazzaroni [71a,71b], B. Le [101], E.M. Le Boulicaut [51], B. Leban [93], A. Lebedev [81], M. LeBlanc [101], F. Ledroit-Guillon [60], A.C.A. Lee [96], S.C. Lee [148], S. Lee [47a,47b], T.F. Lee [92], L.L. Leeuw [33c], H.P. Lefebvre [95], M. Lefebvre [165], C. Leggett [17a], G. Lehmann Miotto [36], M. Leigh [56], W.A. Leight [103], W. Leinonen [113], A. Leisos [152,s], M.A.L. Leite [83c], C.E. Leitgeb [18], R. Leitner [133], K.J.C. Leney [44], T. Lenz [24], S. Leone [74a], C. Leonidopoulos [52], A. Leopold [144], C. Leroy [108], R. Les [107], C.G. Lester [32], M. Levchenko [37], J. Levêque [4], L.J. Levinson [169], G. Levrini [23b,23a], M.P. Lewicki [87], D.J. Lewis [4], A. Li [5], B. Li [62b], C. Li [62a], C-Q. Li [110], H. Li [62a], H. Li [62b], H. Li [14c], H. Li [14b], H. Li [62b], J. Li [62c], K. Li [138], L. Li [62c], M. Li [14a,14e], Q.Y. Li [62a], S. Li [14a,14e], S. Li [62d,62c,d], T. Li [5], X. Li [104], Z. Li [126], Z. Li [104], Z. Li [14a,14e], S. Liang [14a,14e], Z. Liang [14a], M. Liberatore [135], B. Liberti [76a], K. Lie [64c], J. Lieber Marin [83b], H. Lien [68], K. Lin [107], R.E. Lindley [7], J.H. Lindon [2], E. Lipeles [128], A. Lipniacka [16], A. Lister [164], J.D. Little [4], B. Liu [14a], B.X. Liu [142], D. Liu [62d,62c], J.B. Liu [62a], J.K.K. Liu [32], K. Liu [62d,62c], M. Liu [62a], M.Y. Liu [62a], P. Liu [14a], Q. Liu [62d,138,62c], X. Liu [62a], X. Liu [62b], Y. Liu [14d,14e], Y.L. Liu [62b], Y.W. Liu [62a], J. Llorente Merino [142], S.L. Lloyd [94], E.M. Lobodzinska [48], P. Loch [7], T. Lohse [18], K. Lohwasser [139], E. Loiacono [48], M. Lokajicek [131,*], J.D. Lomas [20], J.D. Long [162], I. Longarini [159], L. Longo [70a,70b], R. Longo [162], I. Lopez Paz [67], A. Lopez Solis [48], N. Lorenzo Martinez [4], A.M. Lory [109], G. Löschcke Centeno [146], O. Loseva [37], X. Lou [47a,47b], X. Lou [14a,14e], A. Lounis [66], J. Love [6], P.A. Love [91], G. Lu [14a,14e], M. Lu [80], S. Lu [128], Y.J. Lu [65], H.J. Lubatti [138], C. Luci [75a,75b], F.L. Lucio Alves [14c], F. Luehring [68], I. Luise [145], O. Lukianchuk [66], O. Lundberg [144], B. Lund-Jensen [144], N.A. Luongo [6], M.S. Lutz [36], A.B. Lux [25], D. Lynn [29], R. Lysak [131], E. Lytken [98], V. Lyubushkin [38], T. Lyubushkina [38], M.M. Lyukova [145], H. Ma [29], K. Ma [62a], L.L. Ma [62b], W. Ma [62a], Y. Ma [121], D.M. Mac Donell [165], G. Maccarrone [53], J.C. MacDonald [100], P.C. Machado De Abreu Farias [83b], R. Madar [40], W.F. Mader [50], T. Madula [96], J. Maeda [85], T. Maeno [29], H. Maguire [139], V. Maiboroda [135], A. Maio [130a,130b,130d], K. Maj [86a], O. Majersky [48], S. Majewski [123], N. Makovec [66], V. Maksimovic [15], B. Malaescu [127], Pa. Malecki [87], V.P. Maleev [37], F. Malek [60,o], M. Mali [93], D. Malito [95], U. Mallik [80], S. Maltezos [10], S. Malyukov [38], J. Mamuzic [13], G. Mancini [53], M.N. Mancini [26], G. Manco [73a,73b], J.P. Mandalia [94], I. Mandić [93], L. Manhaes de Andrade Filho [83a], I.M. Maniatis [169], J. Manjarres Ramos [102,ab], D.C. Mankad [169], A. Mann [109], S. Manzoni [36], L. Mao [62c], X. Mapekula [33c], A. Marantis [152,s], G. Marchiori [5], M. Marcisovsky [131], C. Marcon [71a], M. Marinescu [20], S. Marium [48], M. Marjanovic [120], E.J. Marshall [91], Z. Marshall [17a], S. Marti-Garcia [163], T.A. Martin [167], V.J. Martin [52], B. Martin dit Latour [16], L. Martinelli [75a,75b], M. Martinez [13,t], P. Martinez Agullo [163], V.I. Martinez Outschoorn [103], P. Martinez Suarez [13], S. Martin-Haugh [134], V.S. Martoiu [27b], A.C. Martyniuk [96], A. Marzin [36], D. Mascione [78a,78b], L. Masetti [100], T. Mashimo [153], J. Masik [101],

A.L. Maslennikov [37], P. Massarotti [72a,72b], P. Mastrandrea [74a,74b], A. Mastroberardino [43b,43a], T. Masubuchi [153], T. Mathisen [161], J. Matousek [133], N. Matsuzawa [153], J. Maurer [27b], B. Maček [93], D.A. Maximov [37], R. Mazini [148], I. Maznas [152], M. Mazza [107], S.M. Mazza [136], E. Mazzeo [71a,71b], C. Mc Ginn [29], J.P. Mc Gowan [104], S.P. Mc Kee [106], C.C. McCracken [164], E.F. McDonald [105], A.E. McDougall [114], J.A. Mcfayden [146], R.P. McGovern [128], G. Mchedlidze [149b], R.P. Mckenzie [33g], T.C. Mclachlan [48], D.J. Mclaughlin [96], S.J. McMahon [134], C.M. Mcpartland [92], R.A. McPherson [165,x], S. Mehlhase [109], A. Mehta [92], D. Melini [163], B.R. Mellado Garcia [33g], A.H. Melo [55], F. Meloni [48], A.M. Mendes Jacques Da Costa [101], H.Y. Meng [155], L. Meng [91], S. Menke [110], M. Mentink [36], E. Meoni [43b,43a], G. Mercado [115], C. Merlassino [69a,69c], L. Merola [72a,72b], C. Meroni [71a,71b], J. Metcalfe [6], A.S. Mete [6], C. Meyer [68], J-P. Meyer [135], R.P. Middleton [134], L. Mijović [52], G. Mikenberg [169], M. Mikestikova [131], M. Mikuž [93], H. Mildner [100], A. Milic [36], D.W. Miller [39], E.H. Miller [143], L.S. Miller [34], A. Milov [169], D.A. Milstead [47a,47b], T. Min [14c], A.A. Minaenko [37], I.A. Minashvili [149b], L. Mince [59], A.I. Mincer [117], B. Mindur [86a], M. Mineev [38], Y. Mino [88], L.M. Mir [13], M. Miralles Lopez [59], M. Mironova [17a], A. Mishima [153], M.C. Missio [113], A. Mitra [167], V.A. Mitsou [163], Y. Mitsumori [111], O. Miu [155], P.S. Miyagawa [94], T. Mkrtchyan [63a], M. Mlinarevic [96], T. Mlinarevic [96], M. Mlynarikova [36], S. Mobius [19], P. Mogg [109], M.H. Mohamed Farook [112], A.F. Mohammed [14a,14e], S. Mohapatra [41], G. Mokgatitswane [33g], L. Moleri [169], B. Mondal [141], S. Mondal [132], K. Mönig [48], E. Monnier [102], L. Monsonis Romero [163], J. Montejo Berlingen [13], M. Montella [119], F. Montereali [77a,77b], F. Monticelli [90], S. Monzani [69a,69c], N. Morange [66], A.L. Moreira De Carvalho [130a], M. Moreno Llácer [163], C. Moreno Martinez [56], P. Morettini [57b], S. Morgenstern [36], M. Morii [61], M. Morinaga [153], F. Morodei [75a,75b], L. Morvaj [36], P. Moschovakos [36], B. Moser [36], M. Mosidze [149b], T. Moskalets [54], P. Moskvitina [113], J. Moss [31,l], E.J.W. Moyse [103], O. Mtintsilana [33g], S. Muanza [102], J. Mueller [129], D. Muenstermann [91], R. Müller [19], G.A. Mullier [161], A.J. Mullin [32], J.J. Mullin [128], D.P. Mungo [155], D. Munoz Perez [163], F.J. Munoz Sanchez [101], M. Murin [101], W.J. Murray [167,134], M. Muškinja [17a], C. Mwewa [29], A.G. Myagkov [37,a], A.J. Myers [8], G. Myers [68], M. Myska [132], B.P. Nachman [17a], O. Nackenhorst [49], K. Nagai [126], K. Nagano [84], J.L. Nagle [29,aj], E. Nagy [102], A.M. Nairz [36], Y. Nakahama [84], K. Nakamura [84], K. Nakkalil [5], H. Nanjo [124], R. Narayan [44], E.A. Narayanan [112], I. Naryshkin [37], M. Naseri [34], S. Nasri [116b], C. Nass [24], G. Navarro [22a], J. Navarro-Gonzalez [163], R. Nayak [151], A. Nayaz [18], P.Y. Nechaeva [37], F. Nechansky [48], L. Nedic [126], T.J. Neep [20], A. Negri [73a,73b], M. Negrini [23b], C. Nellist [114], C. Nelson [104], K. Nelson [106], S. Nemecek [131], M. Nessi [36,h], M.S. Neubauer [162], F. Neuhaus [100], J. Neundorf [48], R. Newhouse [164], P.R. Newman [20], C.W. Ng [129], Y.W.Y. Ng [48], B. Ngair [116a], H.D.N. Nguyen [108], R.B. Nickerson [126], R. Nicolaidou [135], J. Nielsen [136], M. Niemeyer [55], J. Niermann [55,36], N. Nikiforou [36], V. Nikolaenko [37,a], I. Nikolic-Audit [127], K. Nikolopoulos [20], P. Nilsson [29], I. Ninca [48], H.R. Nindhito [56], G. Ninio [151], A. Nisati [75a], N. Nishu [2], R. Nisius [110], J-E. Nitschke [50], E.K. Nkadimeng [33g], T. Nobe [153], D.L. Noel [32], T. Nommensen [147], M.B. Norfolk [139], R.R.B. Norisam [96], B.J. Norman [34], M. Noury [35a], J. Novak [93], T. Novak [48], L. Novotny [132], R. Novotny [112], L. Nozka [122], K. Ntekas [159], N.M.J. Nunes De Moura Junior [83b], E. Nurse [96], J. Ocariz [127], A. Ochi [85], I. Ochoa [130a], S. Oerdek [48,u], J.T. Offermann [39], A. Ogrodnik [133], A. Oh [101], C.C. Ohm [144], H. Oide [84], R. Oishi [153], M.L. Ojeda [48], Y. Okumura [153], L.F. Oleiro Seabra [130a], S.A. Olivares Pino [137d], D. Oliveira Damazio [29], D. Oliveira Goncalves [83a], J.L. Oliver [159], Ö.O. Öncel [54], A.P. O'Neill [19],

A. Onofre [130a,130c], P.U.E. Onyisi [11], M.J. Oreglia [39], G.E. Orellana [90], D. Orestano [77a,77b], N. Orlando [13], R.S. Orr [155], V. O'Shea [59], L.M. Osojnak [128], R. Ospanov [62a], G. Otero y Garzon [30], H. Otono [89], P.S. Ott [63a], G.J. Ottino [17a], M. Ouchrif [35d], F. Ould-Saada [125], M. Owen [59], R.E. Owen [134], K.Y. Oyulmaz [21a], V.E. Ozcan [21a], F. Ozturk [87], N. Ozturk [8], S. Ozturk [82], H.A. Pacey [126], A. Pacheco Pages [13], C. Padilla Aranda [13], G. Padovano [75a,75b], S. Pagan Griso [17a], G. Palacino [68], A. Palazzo [70a,70b], J. Pan [172], T. Pan [64a], D.K. Panchal [11], C.E. Pandini [114], J.G. Panduro Vazquez [95], H.D. Pandya [1], H. Pang [14b], P. Pani [48], G. Panizzo [69a,69c], L. Paolozzi [56], S. Parajuli [162], A. Paramonov [6], C. Paraskevopoulos [53], D. Paredes Hernandez [64b], K.R. Park [41], T.H. Park [155], M.A. Parker [32], F. Parodi [57b,57a], E.W. Parrish [115], V.A. Parrish [52], J.A. Parsons [41], U. Parzefall [54], B. Pascual Dias [108], L. Pascual Dominguez [151], E. Pasqualucci [75a], S. Passaggio [57b], F. Pastore [95], P. Patel [87], U.M. Patel [51], J.R. Pater [101], T. Pauly [36], J. Pearkes [143], M. Pedersen [125], R. Pedro [130a], S.V. Peleganchuk [37], O. Penc [36], E.A. Pender [52], G.D. Penn [172], K.E. Penski [109], M. Penzin [37], B.S. Peralva [83d], A.P. Pereira Peixoto [60], L. Pereira Sanchez [47a,47b], D.V. Perepelitsa [29,aj], E. Perez Codina [156a], M. Perganti [10], H. Pernegger [36], O. Perrin [40], K. Peters [48], R.F.Y. Peters [101], B.A. Petersen [36], T.C. Petersen [42], E. Petit [102], V. Petousis [132], C. Petridou [152,e], A. Petrukhin [141], M. Pettee [17a], N.E. Pettersson [36], A. Petukhov [37], K. Petukhova [133], R. Pezoa [137f], L. Pezzotti [36], G. Pezzullo [172], T.M. Pham [170], T. Pham [105], P.W. Phillips [134], G. Piacquadio [145], E. Pianori [17a], F. Piazza [123], R. Piegaia [30], D. Pietreanu [27b], A.D. Pilkington [101], M. Pinamonti [69a,69c], J.L. Pinfold [2], B.C. Pinheiro Pereira [130a], A.E. Pinto Pinoargote [100,135], L. Pintucci [69a,69c], K.M. Piper [146], A. Pirttikoski [56], D.A. Pizzi [34], L. Pizzimento [64b], A. Pizzini [114], M.-A. Pleier [29], V. Plesanovs [54], V. Pleskot [133], E. Plotnikova [38], G. Poddar [4], R. Poettgen [98], L. Poggioli [127], I. Pokharel [55], S. Polacek [133], G. Polesello [73a], A. Poley [142,156a], A. Polini [23b], C.S. Pollard [167], Z.B. Pollock [119], E. Pompa Pacchi [75a,75b], D. Ponomarenko [113], L. Pontecorvo [36], S. Popa [27a], G.A. Popeneciu [27d], A. Poreba [36], D.M. Portillo Quintero [156a], S. Pospisil [132], M.A. Postill [139], P. Postolache [27c], K. Potamianos [167], P.A. Potepa [86a], I.N. Potrap [38], C.J. Potter [32], H. Potti [1], T. Poulsen [48], J. Poveda [163], M.E. Pozo Astigarraga [36], A. Prades Ibanez [163], J. Pretel [54], D. Price [101], M. Primavera [70a], M.A. Principe Martin [99], R. Privara [122], T. Procter [59], M.L. Proffitt [138], N. Proklova [128], K. Prokofiev [64c], G. Proto [110], J. Proudfoot [6], M. Przybycien [86a], W.W. Przygoda [86b], A. Psallidas [46], J.E. Puddefoot [139], D. Pudzha [37], D. Pyatiizbyantseva [37], J. Qian [106], D. Qichen [101], Y. Qin [101], T. Qiu [52], A. Quadt [55], M. Queitsch-Maitland [101], G. Quetant [56], R.P. Quinn [164], G. Rabanal Bolanos [61], D. Rafanoharana [54], F. Ragusa [71a,71b], J.L. Rainbolt [39], J.A. Raine [56], S. Rajagopalan [29], E. Ramakoti [37], I.A. Ramirez-Berend [34], K. Ran [48,14e], N.P. Rapheeha [33g], H. Rasheed [27b], V. Raskina [127], D.F. Rassloff [63a], A. Rastogi [17a], S. Rave [100], B. Ravina [55], I. Ravinovich [169], M. Raymond [36], A.L. Read [125], N.P. Readioff [139], D.M. Rebuzzi [73a,73b], G. Redlinger [29], A.S. Reed [110], K. Reeves [26], J.A. Reidelsturz [171], D. Reikher [151], A. Rej [49], C. Rembser [36], A. Renardi [48], M. Renda [27b], M.B. Rendel [110], F. Renner [48], A.G. Rennie [159], A.L. Rescia [48], S. Resconi [71a], M. Ressegotti [57b,57a], S. Rettie [36], J.G. Reyes Rivera [107], E. Reynolds [17a], O.L. Rezanova [37], P. Reznicek [133], N. Ribaric [91], E. Ricci [78a,78b], R. Richter [110], S. Richter [47a,47b], E. Richter-Was [86b], M. Ridel [127], S. Ridouani [35d], P. Rieck [117], P. Riedler [36], E.M. Riefel [47a,47b], J.O. Rieger [114], M. Rijssenbeek [145], A. Rimoldi [73a,73b], M. Rimoldi [36], L. Rinaldi [23b,23a], T.T. Rinn [29], M.P. Rinnagel [109], G. Ripellino [161], I. Riu [13], P. Rivadeneira [48], J.C. Rivera Vergara [165], F. Rizatdinova [121], E. Rizvi [94], B.A. Roberts [167],

B.R. Roberts [17a], S.H. Robertson [104,x], D. Robinson [32], C.M. Robles Gajardo [137f], M. Robles Manzano [100], A. Robson [59], A. Rocchi [76a,76b], C. Roda [74a,74b], S. Rodriguez Bosca [63a], Y. Rodriguez Garcia [22a], A. Rodriguez Rodriguez [54], A.M. Rodríguez Vera [156b], S. Roe [36], J.T. Roemer [159], A.R. Roepe-Gier [136], J. Roggel [171], O. Røhne [125], R.A. Rojas [103], C.P.A. Roland [127], J. Roloff [29], A. Romaniouk [37], E. Romano [73a,73b], M. Romano [23b], A.C. Romero Hernandez [162], N. Rompotis [92], L. Roos [127], S. Rosati [75a], B.J. Rosser [39], E. Rossi [126], E. Rossi [72a,72b], L.P. Rossi [57b], L. Rossini [54], R. Rosten [119], M. Rotaru [27b], B. Rottler [54], C. Rougier [102,ab], D. Rousseau [66], D. Rousso [32], A. Roy [162], S. Roy-Garand [155], A. Rozanov [102], Z.M.A. Rozario [59], Y. Rozen [150], A. Rubio Jimenez [163], A.J. Ruby [92], V.H. Ruelas Rivera [18], T.A. Ruggeri [1], A. Ruggiero [126], A. Ruiz-Martinez [163], A. Rummler [36], Z. Rurikova [54], N.A. Rusakovich [38], H.L. Russell [165], G. Russo [75a,75b], J.P. Rutherfoord [7], S. Rutherford Colmenares [32], K. Rybacki [91], M. Rybar [133], E.B. Rye [125], A. Ryzhov [44], J.A. Sabater Iglesias [56], P. Sabatini [163], H.F-W. Sadrozinski [136], F. Safai Tehrani [75a], B. Safarzadeh Samani [134], M. Safdari [143], S. Saha [165], M. Sahinsoy [110], A. Saibel [163], M. Saimpert [135], M. Saito [153], T. Saito [153], D. Salamani [36], A. Salnikov [143], J. Salt [163], A. Salvador Salas [151], D. Salvatore [43b,43a], F. Salvatore [146], A. Salzburger [36], D. Sammel [54], D. Sampsonidis [152,e], D. Sampsonidou [123], J. Sánchez [163], V. Sanchez Sebastian [163], H. Sandaker [125], C.O. Sander [48], J.A. Sandesara [103], M. Sandhoff [171], C. Sandoval [22b], D.P.C. Sankey [134], T. Sano [88], A. Sansoni [53], L. Santi [75a,75b], C. Santoni [40], H. Santos [130a,130b], A. Santra [169], K.A. Saoucha [160], J.G. Saraiva [130a,130d], J. Sardain [7], O. Sasaki [84], K. Sato [157], C. Sauer [63b], F. Sauerburger [54], E. Sauvan [4], P. Savard [155,ag], R. Sawada [153], C. Sawyer [134], L. Sawyer [97], I. Sayago Galvan [163], C. Sbarra [23b], A. Sbrizzi [23b,23a], T. Scanlon [96], J. Schaarschmidt [138], U. Schäfer [100], A.C. Schaffer [66,44], D. Schaile [109], R.D. Schamberger [145], C. Scharf [18], M.M. Schefer [19], V.A. Schegelsky [37], D. Scheirich [133], F. Schenck [18], M. Schernau [159], C. Scheulen [55], C. Schiavi [57b,57a], E.J. Schioppa [70a,70b], M. Schioppa [43b,43a], B. Schlag [143,n], K.E. Schleicher [54], S. Schlenker [36], J. Schmeing [171], M.A. Schmidt [171], K. Schmieden [100], C. Schmitt [100], N. Schmitt [100], S. Schmitt [48], L. Schoeffel [135], A. Schoening [63b], P.G. Scholer [54], E. Schopf [126], M. Schott [100], J. Schovancova [36], S. Schramm [56], T. Schroer [56], H-C. Schultz-Coulon [63a], M. Schumacher [54], B.A. Schumm [136], Ph. Schune [135], A.J. Schuy [138], H.R. Schwartz [136], A. Schwartzman [143], T.A. Schwarz [106], Ph. Schwemling [135], R. Schwienhorst [107], A. Sciandra [136], G. Sciolla [26], F. Scuri [74a], C.D. Sebastiani [92], K. Sedlaczek [115], P. Seema [18], S.C. Seidel [112], A. Seiden [136], B.D. Seidlitz [41], C. Seitz [48], J.M. Seixas [83b], G. Sekhniaidze [72a], L. Selem [60], N. Semprini-Cesari [23b,23a], D. Sengupta [56], V. Senthilkumar [163], L. Serin [66], L. Serkin [69a,69b], M. Sessa [76a,76b], H. Severini [120], F. Sforza [57b,57a], A. Sfyrla [56], E. Shabalina [55], R. Shaheen [144], J.D. Shahinian [128], D. Shaked Renous [169], L.Y. Shan [14a], M. Shapiro [17a], A. Sharma [36], A.S. Sharma [164], P. Sharma [80], P.B. Shatalov [37], K. Shaw [146], S.M. Shaw [101], A. Shcherbakova [37], Q. Shen [62c,5], D.J. Sheppard [142], P. Sherwood [96], L. Shi [96], X. Shi [14a], C.O. Shimmin [172], J.D. Shinner [95], I.P.J. Shipsey [126], S. Shirabe [89], M. Shiyakova [38,v], J. Shlomi [169], M.J. Shochet [39], J. Shojaii [105], D.R. Shope [125], B. Shrestha [120], S. Shrestha [119,ak], E.M. Shrif [33g], M.J. Shroff [165], P. Sicho [131], A.M. Sickles [162], E. Sideras Haddad [33g], A. Sidoti [23b], F. Siegert [50], Dj. Sijacki [15], F. Sili [90], J.M. Silva [20], M.V. Silva Oliveira [29], S.B. Silverstein [47a], S. Simion [66], R. Simoniello [36], E.L. Simpson [59], H. Simpson [146], L.R. Simpson [106], N.D. Simpson [98], S. Simsek [82], S. Sindhu [55], P. Sinervo [155], S. Singh [155], S. Sinha [48], S. Sinha [101], M. Sioli [23b,23a], I. Siral [36], E. Sitnikova [48],

S.Yu. Sivoklokov [37,*], J. Sjölin [47a,47b], A. Skaf [55], E. Skorda [20], P. Skubic [120], M. Slawinska [87], V. Smakhtin [169], B.H. Smart [134], S.Yu. Smirnov [37], Y. Smirnov [37], L.N. Smirnova [37,a], O. Smirnova [98], A.C. Smith [41], E.A. Smith [39], H.A. Smith [126], J.L. Smith [92], R. Smith [143], M. Smizanska [91], K. Smolek [132], A.A. Snesarev [37], S.R. Snider [155], H.L. Snoek [114], S. Snyder [29], R. Sobie [165,x], A. Soffer [151], C.A. Solans Sanchez [36], E.Yu. Soldatov [37], U. Soldevila [163], A.A. Solodkov [37], S. Solomon [26], A. Soloshenko [38], K. Solovieva [54], O.V. Solovyanov [40], V. Solovyev [37], P. Sommer [36], A. Sonay [13], W.Y. Song [156b], A. Sopczak [132], A.L. Sopio [96], F. Sopkova [28b], J.D. Sorenson [112], I.R. Sotarriva Alvarez [154], V. Sothilingam [63a], O.J. Soto Sandoval [137c,137b], S. Sottocornola [68], R. Soualah [160], Z. Soumaimi [35e], D. South [48], N. Soybelman [169], S. Spagnolo [70a,70b], M. Spalla [110], D. Sperlich [54], G. Spigo [36], S. Spinali [91], D.P. Spiteri [59], M. Spousta [133], E.J. Staats [34], R. Stamen [63a], A. Stampekis [20], M. Standke [24], E. Stanecka [87], M.V. Stange [50], B. Stanislaus [17a], M.M. Stanitzki [48], B. Stapf [48], E.A. Starchenko [37], G.H. Stark [136], J. Stark [102,ab], P. Staroba [131], P. Starovoitov [63a], S. Stärz [104], R. Staszewski [87], G. Stavropoulos [46], J. Steentoft [161], P. Steinberg [29], B. Stelzer [142,156a], H.J. Stelzer [129], O. Stelzer-Chilton [156a], H. Stenzel [58], T.J. Stevenson [146], G.A. Stewart [36], J.R. Stewart [121], M.C. Stockton [36], G. Stoicea [27b], M. Stolarski [130a], S. Stonjek [110], A. Straessner [50], J. Strandberg [144], S. Strandberg [47a,47b], M. Stratmann [171], M. Strauss [120], T. Strebler [102], P. Strizenec [28b], R. Ströhmer [166], D.M. Strom [123], R. Stroynowski [44], A. Strubig [47a,47b], S.A. Stucci [29], B. Stugu [16], J. Stupak [120], N.A. Styles [48], D. Su [143], S. Su [62a], W. Su [62d], X. Su [62a,66], K. Sugizaki [153], V.V. Sulin [37], M.J. Sullivan [92], D.M.S. Sultan [78a,78b], L. Sultanaliyeva [37], S. Sultansoy [3b], T. Sumida [88], S. Sun [106], S. Sun [170], O. Sunneborn Gudnadottir [161], N. Sur [102], M.R. Sutton [146], H. Suzuki [157], M. Svatos [131], M. Swiatlowski [156a], T. Swirski [166], I. Sykora [28a], M. Sykora [133], T. Sykora [133], D. Ta [100], K. Tackmann [48,u], A. Taffard [159], R. Tafirout [156a], J.S. Tafoya Vargas [66], Y. Takubo [84], M. Talby [102], A.A. Talyshev [37], K.C. Tam [64b], N.M. Tamir [151], A. Tanaka [153], J. Tanaka [153], R. Tanaka [66], M. Tanasini [57b,57a], Z. Tao [164], S. Tapia Araya [137f], S. Tapprogge [100], A. Tarek Abouelfadl Mohamed [107], S. Tarem [150], K. Tariq [14a], G. Tarna [102,27b], G.F. Tartarelli [71a], P. Tas [133], M. Tasevsky [131], E. Tassi [43b,43a], A.C. Tate [162], G. Tateno [153], Y. Tayalati [35e,w], G.N. Taylor [105], W. Taylor [156b], A.S. Tee [170], R. Teixeira De Lima [143], P. Teixeira-Dias [95], J.J. Teoh [155], K. Terashi [153], J. Terron [99], S. Terzo [13], M. Testa [53], R.J. Teuscher [155,x], A. Thaler [79], O. Theiner [56], N. Themistokleous [52], T. Theveneaux-Pelzer [102], O. Thielmann [171], D.W. Thomas [95], J.P. Thomas [20], E.A. Thompson [17a], P.D. Thompson [20], E. Thomson [128], Y. Tian [55], V. Tikhomirov [37,a], Yu.A. Tikhonov [37], S. Timoshenko [37], D. Timoshyn [133], E.X.L. Ting [1], P. Tipton [172], S.H. Tlou [33g], A. Tnourji [40], K. Todome [154], S. Todorova-Nova [133], S. Todt [50], M. Togawa [84], J. Tojo [89], S. Tokár [28a], K. Tokushuku [84], O. Toldaiev [68], R. Tombs [32], M. Tomoto [84,111], L. Tompkins [143,n], K.W. Topolnicki [86b], E. Torrence [123], H. Torres [102,ab], E. Torró Pastor [163], M. Toscani [30], C. Tosciri [39], M. Tost [11], D.R. Tovey [139], A. Traeet [16], I.S. Trandafir [27b], T. Trefzger [166], A. Tricoli [29], I.M. Trigger [156a], S. Trincaz-Duvoid [127], D.A. Trischuk [26], B. Trocmé [60], C. Troncon [71a], L. Truong [33c], M. Trzebinski [87], A. Trzupek [87], F. Tsai [145], M. Tsai [106], A. Tsiamis [152,e], P.V. Tsiareshka [37], S. Tsigaridas [156a], A. Tsirigotis [152,s], V. Tsiskaridze [155], E.G. Tskhadadze [149a], M. Tsopoulou [152,e], Y. Tsujikawa [88], I.I. Tsukerman [37], V. Tsulaia [17a], S. Tsuno [84], K. Tsuri [118], D. Tsybychev [145], Y. Tu [64b], A. Tudorache [27b], V. Tudorache [27b], A.N. Tuna [61], S. Turchikhin [57b,57a], I. Turk Cakir [3a], R. Turra [71a],

T. Turtuvshin [38,y], P.M. Tuts [41], S. Tzamarias [152,e], P. Tzanis [10], E. Tzovara [100], F. Ukegawa [157], P.A. Ulloa Poblete [137c,137b], E.N. Umaka [29], G. Unal [36], M. Unal [11], A. Undrus [29], G. Unel [159], J. Urban [28b], P. Urquijo [105], P. Urrejola [137a], G. Usai [8], R. Ushioda [154], M. Usman [108], Z. Uysal [82], V. Vacek [132], B. Vachon [104], K.O.H. Vadla [125], T. Vafeiadis [36], A. Vaitkus [96], C. Valderanis [109], E. Valdes Santurio [47a,47b], M. Valente [156a], S. Valentinetti [23b,23a], A. Valero [163], E. Valiente Moreno [163], A. Vallier [102,ab], J.A. Valls Ferrer [163], D.R. Van Arneman [114], T.R. Van Daalen [138], A. Van Der Graaf [49], P. Van Gemmeren [6], M. Van Rijnbach [125,36], S. Van Stroud [96], I. Van Vulpen [114], M. Vanadia [76a,76b], W. Vandelli [36], E.R. Vandewall [121], D. Vannicola [151], L. Vannoli [57b,57a], R. Vari [75a], E.W. Varnes [7], C. Varni [17b], T. Varol [148], D. Varouchas [66], L. Varriale [163], K.E. Varvell [147], M.E. Vasile [27b], L. Vaslin [84], G.A. Vasquez [165], A. Vasyukov [38], F. Vazeille [40], T. Vazquez Schroeder [36], J. Veatch [31], V. Vecchio [101], M.J. Veen [103], I. Veliscek [126], L.M. Veloce [155], F. Veloso [130a,130c], S. Veneziano [75a], A. Ventura [70a,70b], S. Ventura Gonzalez [135], A. Verbytskyi [110], M. Verducci [74a,74b], C. Vergis [24], M. Verissimo De Araujo [83b], W. Verkerke [114], J.C. Vermeulen [114], C. Vernieri [143], M. Vessella [103], M.C. Vetterli [142,ag], A. Vgenopoulos [152,e], N. Viaux Maira [137f], T. Vickey [139], O.E. Vickey Boeriu [139], G.H.A. Viehhauser [126], L. Vigani [63b], M. Villa [23b,23a], M. Villaplana Perez [163], E.M. Villhauer [52], E. Vilucchi [53], M.G. Vincter [34], G.S. Virdee [20], A. Vishwakarma [52], A. Visibile [114], C. Vittori [36], I. Vivarelli [146], E. Voevodina [110], F. Vogel [109], J.C. Voigt [50], P. Vokac [132], Yu. Volkotrub [86a], J. Von Ahnen [48], E. Von Toerne [24], B. Vormwald [36], V. Vorobel [133], K. Vorobev [37], M. Vos [163], K. Voss [141], M. Vozak [114], L. Vozdecky [94], N. Vranjes [15], M. Vranjes Milosavljevic [15], M. Vreeswijk [114], N.K. Vu [62d,62c], R. Vuillermet [36], O. Vujinovic [100], I. Vukotic [39], S. Wada [157], C. Wagner [103], J.M. Wagner [17a], W. Wagner [171], S. Wahdan [171], H. Wahlberg [90], M. Wakida [111], J. Walder [134], R. Walker [109], W. Walkowiak [141], A. Wall [128], T. Wamorkar [6], A.Z. Wang [136], C. Wang [100], C. Wang [11], H. Wang [17a], J. Wang [64c], R.-J. Wang [100], R. Wang [61], R. Wang [6], S.M. Wang [148], S. Wang [62b], T. Wang [62a], W.T. Wang [80], W. Wang [14a], X. Wang [14c], X. Wang [162], X. Wang [62c], Y. Wang [62d], Y. Wang [14c], Z. Wang [106], Z. Wang [62d,51,62c], Z. Wang [106], A. Warburton [104], R.J. Ward [20], N. Warrack [59], S. Waterhouse [95], A.T. Watson [20], H. Watson [59], M.F. Watson [20], E. Watton [59,134], G. Watts [138], B.M. Waugh [96], C. Weber [29], H.A. Weber [18], M.S. Weber [19], S.M. Weber [63a], C. Wei [62a], Y. Wei [126], A.R. Weidberg [126], E.J. Weik [117], J. Weingarten [49], M. Weirich [100], C. Weiser [54], C.J. Wells [48], T. Wenaus [29], B. Wendland [49], T. Wengler [36], N.S. Wenke [110], N. Wermes [24], M. Wessels [63a], A.M. Wharton [91], A.S. White [61], A. White [8], M.J. White [1], D. Whiteson [159], L. Wickremasinghe [124], W. Wiedenmann [170], M. Wielers [134], C. Wiglesworth [42], D.J. Wilbern [120], H.G. Wilkens [36], D.M. Williams [41], H.H. Williams [128], S. Williams [32], S. Willocq [103], B.J. Wilson [101], P.J. Windischhofer [39], F.I. Winkel [30], F. Winklmeier [123], B.T. Winter [54], J.K. Winter [101], M. Wittgen [143], M. Wobisch [97], Z. Wolffs [114], J. Wollrath [159], M.W. Wolter [87], H. Wolters [130a,130c], E.L. Woodward [41], S.D. Worm [48], B.K. Wosiek [87], K.W. Woźniak [87], S. Wozniewski [55], K. Wraight [59], C. Wu [20], J. Wu [14a,14e], M. Wu [64a], M. Wu [113], S.L. Wu [170], X. Wu [56], Y. Wu [62a], Z. Wu [135], J. Wuerzinger [110,ae], T.R. Wyatt [101], B.M. Wynne [52], S. Xella [42], L. Xia [14c], M. Xia [14b], J. Xiang [64c], M. Xie [62a], X. Xie [62a], S. Xin [14a,14e], A. Xiong [123], J. Xiong [17a], D. Xu [14a], H. Xu [62a], L. Xu [62a], R. Xu [128], T. Xu [106], Y. Xu [14b], Z. Xu [52], Z. Xu [14c], B. Yabsley [147], S. Yacoob [33a], Y. Yamaguchi [154], E. Yamashita [153], H. Yamauchi [157], T. Yamazaki [17a], Y. Yamazaki [85], J. Yan [62c], S. Yan [126], Z. Yan [25], H.J. Yang [62c,62d], H.T. Yang [62a], S. Yang [62a], T. Yang [64c], X. Yang [36], X. Yang [14a], Y. Yang [44], Y. Yang [62a], Z. Yang [62a], W-M. Yao [17a], H. Ye [14c],

H. Ye [55], J. Ye [14a], S. Ye [29], X. Ye [62a], Y. Yeh [96], I. Yeletskikh [38], B.K. Yeo [17b], M.R. Yexley [96], P. Yin [41], K. Yorita [168], S. Younas [27b], C.J.S. Young [36], C. Young [143], C. Yu [14a,14e,ai], Y. Yu [62a], M. Yuan [106], R. Yuan [62b], L. Yue [96], M. Zaazoua [62a], B. Zabinski [87], E. Zaid [52], Z.K. Zak [87], T. Zakareishvili [163], N. Zakharchuk [34], S. Zambito [56], J.A. Zamora Saa [137d,137b], J. Zang [153], D. Zanzi [54], O. Zaplatilek [132], C. Zeitnitz [171], H. Zeng [14a], J.C. Zeng [162], D.T. Zenger Jr [26], O. Zenin [37], T. Ženiš [28a], S. Zenz [94], S. Zerradi [35a], D. Zerwas [66], M. Zhai [14a,14e], D.F. Zhang [139], J. Zhang [62b], J. Zhang [6], K. Zhang [14a,14e], L. Zhang [14c], P. Zhang [14a,14e], R. Zhang [170], S. Zhang [106], S. Zhang [44], T. Zhang [153], X. Zhang [62c], X. Zhang [62b], Y. Zhang [62c,5], Y. Zhang [96], Y. Zhang [14c], Z. Zhang [17a], Z. Zhang [66], H. Zhao [138], T. Zhao [62b], Y. Zhao [136], Z. Zhao [62a], A. Zhemchugov [38], J. Zheng [14c], K. Zheng [162], X. Zheng [62a], Z. Zheng [143], D. Zhong [162], B. Zhou [106], H. Zhou [7], N. Zhou [62c], Y. Zhou [14c], Y. Zhou [7], C.G. Zhu [62b], J. Zhu [106], Y. Zhu [62c], Y. Zhu [62a], X. Zhuang [14a], K. Zhukov [37], V. Zhulanov [37], N.I. Zimine [38], J. Zinsser [63b], M. Ziolkowski [141], L. Živković [15], A. Zoccoli [23b,23a], K. Zoch [61], T.G. Zorbas [139], O. Zormpa [46], W. Zou [41], L. Zwalinski [36]

[1] *Department of Physics, University of Adelaide, Adelaide; Australia*
[2] *Department of Physics, University of Alberta, Edmonton AB; Canada*
[3] [(a)] *Department of Physics, Ankara University, Ankara;* [(b)] *Division of Physics, TOBB University of Economics and Technology, Ankara; Türkiye*
[4] *LAPP, Université Savoie Mont Blanc, CNRS/IN2P3, Annecy; France*
[5] *APC, Université Paris Cité, CNRS/IN2P3, Paris; France*
[6] *High Energy Physics Division, Argonne National Laboratory, Argonne IL; United States of America*
[7] *Department of Physics, University of Arizona, Tucson AZ; United States of America*
[8] *Department of Physics, University of Texas at Arlington, Arlington TX; United States of America*
[9] *Physics Department, National and Kapodistrian University of Athens, Athens; Greece*
[10] *Physics Department, National Technical University of Athens, Zografou; Greece*
[11] *Department of Physics, University of Texas at Austin, Austin TX; United States of America*
[12] *Institute of Physics, Azerbaijan Academy of Sciences, Baku; Azerbaijan*
[13] *Institut de Física d'Altes Energies (IFAE), Barcelona Institute of Science and Technology, Barcelona; Spain*
[14] [(a)] *Institute of High Energy Physics, Chinese Academy of Sciences, Beijing;* [(b)] *Physics Department, Tsinghua University, Beijing;* [(c)] *Department of Physics, Nanjing University, Nanjing;* [(d)] *School of Science, Shenzhen Campus of Sun Yat-sen University;* [(e)] *University of Chinese Academy of Science (UCAS), Beijing; China*
[15] *Institute of Physics, University of Belgrade, Belgrade; Serbia*
[16] *Department for Physics and Technology, University of Bergen, Bergen; Norway*
[17] [(a)] *Physics Division, Lawrence Berkeley National Laboratory, Berkeley CA;* [(b)] *University of California, Berkeley CA; United States of America*
[18] *Institut für Physik, Humboldt Universität zu Berlin, Berlin; Germany*
[19] *Albert Einstein Center for Fundamental Physics and Laboratory for High Energy Physics, University of Bern, Bern; Switzerland*
[20] *School of Physics and Astronomy, University of Birmingham, Birmingham; United Kingdom*
[21] [(a)] *Department of Physics, Bogazici University, Istanbul;* [(b)] *Department of Physics Engineering, Gaziantep University, Gaziantep;* [(c)] *Department of Physics, Istanbul University, Istanbul; Türkiye*
[22] [(a)] *Facultad de Ciencias y Centro de Investigaciónes, Universidad Antonio Nariño, Bogotá;* [(b)] *Departamento de Física, Universidad Nacional de Colombia, Bogotá; Colombia*
[23] [(a)] *Dipartimento di Fisica e Astronomia A. Righi, Università di Bologna, Bologna;* [(b)] *INFN Sezione di Bologna; Italy*
[24] *Physikalisches Institut, Universität Bonn, Bonn; Germany*
[25] *Department of Physics, Boston University, Boston MA; United States of America*
[26] *Department of Physics, Brandeis University, Waltham MA; United States of America*
[27] [(a)] *Transilvania University of Brasov, Brasov;* [(b)] *Horia Hulubei National Institute of Physics and Nuclear Engineering, Bucharest;* [(c)] *Department of Physics, Alexandru Ioan Cuza University of Iasi, Iasi;* [(d)] *National Institute for Research and Development of Isotopic and Molecular Technologies, Physics Department, Cluj-Napoca;* [(e)] *National University of Science and Technology Politechnica, Bucharest;* [(f)] *West University in Timisoara, Timisoara;* [(g)] *Faculty of Physics, University of Bucharest, Bucharest; Romania*
[28] [(a)] *Faculty of Mathematics, Physics and Informatics, Comenius University, Bratislava;* [(b)] *Department of Subnuclear Physics, Institute of Experimental Physics of the Slovak Academy of Sciences, Kosice; Slovak Republic*
[29] *Physics Department, Brookhaven National Laboratory, Upton NY; United States of America*
[30] *Universidad de Buenos Aires, Facultad de Ciencias Exactas y Naturales, Departamento de Física, y CONICET, Instituto de Física de Buenos Aires (IFIBA), Buenos Aires; Argentina*
[31] *California State University, CA; United States of America*
[32] *Cavendish Laboratory, University of Cambridge, Cambridge; United Kingdom*
[33] [(a)] *Department of Physics, University of Cape Town, Cape Town;* [(b)] *iThemba Labs, Western Cape;* [(c)] *Department of Mechanical Engineering Science, University of Johannesburg, Johannesburg;* [(d)] *National Institute of Physics, University of the Philippines Diliman (Philippines);* [(e)] *University of South Africa, Department of Physics, Pretoria;* [(f)] *University of Zululand, KwaDlangezwa;* [(g)] *School of Physics, University of the Witwatersrand, Johannesburg; South Africa*
[34] *Department of Physics, Carleton University, Ottawa ON; Canada*
[35] [(a)] *Faculté des Sciences Ain Chock, Réseau Universitaire de Physique des Hautes Energies - Université Hassan II, Casablanca;* [(b)] *Faculté des Sciences, Université Ibn-Tofail, Kénitra;* [(c)] *Faculté des Sciences Semlalia, Université Cadi Ayyad, LPHEA-Marrakech;* [(d)] *LPMR, Faculté des Sciences, Université Mohamed Premier, Oujda;* [(e)] *Faculté des sciences, Université Mohammed V, Rabat;* [(f)] *Institute of Applied Physics, Mohammed VI Polytechnic University, Ben Guerir; Morocco*
[36] *CERN, Geneva; Switzerland*
[37] *Affiliated with an institute covered by a cooperation agreement with CERN*
[38] *Affiliated with an international laboratory covered by a cooperation agreement with CERN*
[39] *Enrico Fermi Institute, University of Chicago, Chicago IL; United States of America*
[40] *LPC, Université Clermont Auvergne, CNRS/IN2P3, Clermont-Ferrand; France*
[41] *Nevis Laboratory, Columbia University, Irvington NY; United States of America*
[42] *Niels Bohr Institute, University of Copenhagen, Copenhagen; Denmark*
[43] [(a)] *Dipartimento di Fisica, Università della Calabria, Rende;* [(b)] *INFN Gruppo Collegato di Cosenza, Laboratori Nazionali di Frascati; Italy*
[44] *Physics Department, Southern Methodist University, Dallas TX; United States of America*
[45] *Physics Department, University of Texas at Dallas, Richardson TX; United States of America*
[46] *National Centre for Scientific Research "Demokritos", Agia Paraskevi; Greece*
[47] [(a)] *Department of Physics, Stockholm University;* [(b)] *Oskar Klein Centre, Stockholm; Sweden*

[48] Deutsches Elektronen-Synchrotron DESY, Hamburg and Zeuthen; Germany
[49] Fakultät Physik , Technische Universität Dortmund, Dortmund; Germany
[50] Institut für Kern- und Teilchenphysik, Technische Universität Dresden, Dresden; Germany
[51] Department of Physics, Duke University, Durham NC; United States of America
[52] SUPA - School of Physics and Astronomy, University of Edinburgh, Edinburgh; United Kingdom
[53] INFN e Laboratori Nazionali di Frascati, Frascati; Italy
[54] Physikalisches Institut, Albert-Ludwigs-Universität Freiburg, Freiburg; Germany
[55] II. Physikalisches Institut, Georg-August-Universität Göttingen, Göttingen; Germany
[56] Département de Physique Nucléaire et Corpusculaire, Université de Genève, Genève; Switzerland
[57] [(a)] Dipartimento di Fisica, Università di Genova, Genova; [(b)] INFN Sezione di Genova; Italy
[58] II. Physikalisches Institut, Justus-Liebig-Universität Giessen, Giessen; Germany
[59] SUPA - School of Physics and Astronomy, University of Glasgow, Glasgow; United Kingdom
[60] LPSC, Université Grenoble Alpes, CNRS/IN2P3, Grenoble INP, Grenoble; France
[61] Laboratory for Particle Physics and Cosmology, Harvard University, Cambridge MA; United States of America
[62] [(a)] Department of Modern Physics and State Key Laboratory of Particle Detection and Electronics, University of Science and Technology of China, Hefei; [(b)] Institute of Frontier and Interdisciplinary Science and Key Laboratory of Particle Physics and Particle Irradiation (MOE), Shandong University, Qingdao; [(c)] School of Physics and Astronomy, Shanghai Jiao Tong University, Key Laboratory for Particle Astrophysics and Cosmology (MOE), SKLPPC, Shanghai; [(d)] Tsung-Dao Lee Institute, Shanghai; [(e)] School of Physics and Microelectronics, Zhengzhou University; China
[63] [(a)] Kirchhoff-Institut für Physik, Ruprecht-Karls-Universität Heidelberg, Heidelberg; [(b)] Physikalisches Institut, Ruprecht-Karls-Universität Heidelberg, Heidelberg; Germany
[64] [(a)] Department of Physics, Chinese University of Hong Kong, Shatin, N.T., Hong Kong; [(b)] Department of Physics, University of Hong Kong, Hong Kong; [(c)] Department of Physics and Institute for Advanced Study, Hong Kong University of Science and Technology, Clear Water Bay, Kowloon, Hong Kong; China
[65] Department of Physics, National Tsing Hua University, Hsinchu; Taiwan
[66] IJCLab, Université Paris-Saclay, CNRS/IN2P3, 91405, Orsay; France
[67] Centro Nacional de Microelectrónica (IMB-CNM-CSIC), Barcelona; Spain
[68] Department of Physics, Indiana University, Bloomington IN; United States of America
[69] [(a)] INFN Gruppo Collegato di Udine, Sezione di Trieste, Udine; [(b)] ICTP, Trieste; [(c)] Dipartimento Politecnico di Ingegneria e Architettura, Università di Udine, Udine; Italy
[70] [(a)] INFN Sezione di Lecce; [(b)] Dipartimento di Matematica e Fisica, Università del Salento, Lecce; Italy
[71] [(a)] INFN Sezione di Milano; [(b)] Dipartimento di Fisica, Università di Milano, Milano; Italy
[72] [(a)] INFN Sezione di Napoli; [(b)] Dipartimento di Fisica, Università di Napoli, Napoli; Italy
[73] [(a)] INFN Sezione di Pavia; [(b)] Dipartimento di Fisica, Università di Pavia, Pavia; Italy
[74] [(a)] INFN Sezione di Pisa; [(b)] Dipartimento di Fisica E. Fermi, Università di Pisa, Pisa; Italy
[75] [(a)] INFN Sezione di Roma; [(b)] Dipartimento di Fisica, Sapienza Università di Roma, Roma; Italy
[76] [(a)] INFN Sezione di Roma Tor Vergata; [(b)] Dipartimento di Fisica, Università di Roma Tor Vergata, Roma; Italy
[77] [(a)] INFN Sezione di Roma Tre; [(b)] Dipartimento di Matematica e Fisica, Università Roma Tre, Roma; Italy
[78] [(a)] INFN-TIFPA; [(b)] Università degli Studi di Trento, Trento; Italy
[79] Universität Innsbruck, Department of Astro and Particle Physics, Innsbruck; Austria
[80] University of Iowa, Iowa City IA; United States of America
[81] Department of Physics and Astronomy, Iowa State University, Ames IA; United States of America
[82] Istinye University, Sariyer, Istanbul; Türkiye
[83] [(a)] Departamento de Engenharia Elétrica, Universidade Federal de Juiz de Fora (UFJF), Juiz de Fora; [(b)] Universidade Federal do Rio De Janeiro COPPE/EE/IF, Rio de Janeiro; [(c)] Instituto de Física, Universidade de São Paulo, São Paulo; [(d)] Rio de Janeiro State University, Rio de Janeiro; Brazil
[84] KEK, High Energy Accelerator Research Organization, Tsukuba; Japan
[85] Graduate School of Science, Kobe University, Kobe; Japan
[86] [(a)] AGH University of Krakow, Faculty of Physics and Applied Computer Science, Krakow; [(b)] Marian Smoluchowski Institute of Physics, Jagiellonian University, Krakow; Poland
[87] Institute of Nuclear Physics Polish Academy of Sciences, Krakow; Poland
[88] Faculty of Science, Kyoto University, Kyoto; Japan
[89] Research Center for Advanced Particle Physics and Department of Physics, Kyushu University, Fukuoka; Japan
[90] Instituto de Física La Plata, Universidad Nacional de La Plata and CONICET, La Plata; Argentina
[91] Physics Department, Lancaster University, Lancaster; United Kingdom
[92] Oliver Lodge Laboratory, University of Liverpool, Liverpool; United Kingdom
[93] Department of Experimental Particle Physics, Jožef Stefan Institute and Department of Physics, University of Ljubljana, Ljubljana; Slovenia
[94] School of Physics and Astronomy, Queen Mary University of London, London; United Kingdom
[95] Department of Physics, Royal Holloway University of London, Egham; United Kingdom
[96] Department of Physics and Astronomy, University College London, London; United Kingdom
[97] Louisiana Tech University, Ruston LA; United States of America
[98] Fysiska institutionen, Lunds universitet, Lund; Sweden
[99] Departamento de Física Teorica C-15 and CIAFF, Universidad Autónoma de Madrid, Madrid; Spain
[100] Institut für Physik, Universität Mainz, Mainz; Germany
[101] School of Physics and Astronomy, University of Manchester, Manchester; United Kingdom
[102] CPPM, Aix-Marseille Université, CNRS/IN2P3, Marseille; France
[103] Department of Physics, University of Massachusetts, Amherst MA; United States of America
[104] Department of Physics, McGill University, Montreal QC; Canada
[105] School of Physics, University of Melbourne, Victoria; Australia
[106] Department of Physics, University of Michigan, Ann Arbor MI; United States of America
[107] Department of Physics and Astronomy, Michigan State University, East Lansing MI; United States of America
[108] Group of Particle Physics, University of Montreal, Montreal QC; Canada
[109] Fakultät für Physik, Ludwig-Maximilians-Universität München, München; Germany
[110] Max-Planck-Institut für Physik (Werner-Heisenberg-Institut), München; Germany
[111] Graduate School of Science and Kobayashi-Maskawa Institute, Nagoya University, Nagoya; Japan
[112] Department of Physics and Astronomy, University of New Mexico, Albuquerque NM; United States of America
[113] Institute for Mathematics, Astrophysics and Particle Physics, Radboud University/Nikhef, Nijmegen; Netherlands
[114] Nikhef National Institute for Subatomic Physics and University of Amsterdam, Amsterdam; Netherlands
[115] Department of Physics, Northern Illinois University, DeKalb IL; United States of America
[116] [(a)] New York University Abu Dhabi, Abu Dhabi; [(b)] United Arab Emirates University, Al Ain; United Arab Emirates
[117] Department of Physics, New York University, New York NY; United States of America
[118] Ochanomizu University, Otsuka, Bunkyo-ku, Tokyo; Japan
[119] Ohio State University, Columbus OH; United States of America
[120] Homer L. Dodge Department of Physics and Astronomy, University of Oklahoma, Norman OK; United States of America
[121] Department of Physics, Oklahoma State University, Stillwater OK; United States of America
[122] Palacký University, Joint Laboratory of Optics, Olomouc; Czech Republic

[123] Institute for Fundamental Science, University of Oregon, Eugene, OR; United States of America
[124] Graduate School of Science, Osaka University, Osaka; Japan
[125] Department of Physics, University of Oslo, Oslo; Norway
[126] Department of Physics, Oxford University, Oxford; United Kingdom
[127] LPNHE, Sorbonne Université, Université Paris Cité, CNRS/IN2P3, Paris; France
[128] Department of Physics, University of Pennsylvania, Philadelphia PA; United States of America
[129] Department of Physics and Astronomy, University of Pittsburgh, Pittsburgh PA; United States of America
[130] [(a)] Laboratório de Instrumentação e Física Experimental de Partículas - LIP, Lisboa; [(b)] Departamento de Física, Faculdade de Ciências, Universidade de Lisboa, Lisboa; [(c)] Departamento de Física, Universidade de Coimbra, Coimbra; [(d)] Centro de Física Nuclear da Universidade de Lisboa, Lisboa; [(e)] Departamento de Física, Universidade do Minho, Braga; [(f)] Departamento de Física Teórica y del Cosmos, Universidad de Granada, Granada (Spain); [(g)] Departamento de Física, Instituto Superior Técnico, Universidade de Lisboa, Lisboa; Portugal
[131] Institute of Physics of the Czech Academy of Sciences, Prague; Czech Republic
[132] Czech Technical University in Prague, Prague; Czech Republic
[133] Charles University, Faculty of Mathematics and Physics, Prague; Czech Republic
[134] Particle Physics Department, Rutherford Appleton Laboratory, Didcot; United Kingdom
[135] IRFU, CEA, Université Paris-Saclay, Gif-sur-Yvette; France
[136] Santa Cruz Institute for Particle Physics, University of California Santa Cruz, Santa Cruz CA; United States of America
[137] [(a)] Departamento de Física, Pontificia Universidad Católica de Chile, Santiago; [(b)] Millennium Institute for Subatomic physics at high energy frontier (SAPHIR), Santiago; [(c)] Instituto de Investigación Multidisciplinario en Ciencia y Tecnología, y Departamento de Física, Universidad de La Serena; [(d)] Universidad Andres Bello, Department of Physics, Santiago; [(e)] Instituto de Alta Investigación, Universidad de Tarapacá, Arica; [(f)] Departamento de Física, Universidad Técnica Federico Santa María, Valparaíso; Chile
[138] Department of Physics, University of Washington, Seattle WA; United States of America
[139] Department of Physics and Astronomy, University of Sheffield, Sheffield; United Kingdom
[140] Department of Physics, Shinshu University, Nagano; Japan
[141] Department Physik, Universität Siegen, Siegen; Germany
[142] Department of Physics, Simon Fraser University, Burnaby BC; Canada
[143] SLAC National Accelerator Laboratory, Stanford CA; United States of America
[144] Department of Physics, Royal Institute of Technology, Stockholm; Sweden
[145] Departments of Physics and Astronomy, Stony Brook University, Stony Brook NY; United States of America
[146] Department of Physics and Astronomy, University of Sussex, Brighton; United Kingdom
[147] School of Physics, University of Sydney, Sydney; Australia
[148] Institute of Physics, Academia Sinica, Taipei; Taiwan
[149] [(a)] E. Andronikashvili Institute of Physics, Iv. Javakhishvili Tbilisi State University, Tbilisi; [(b)] High Energy Physics Institute, Tbilisi State University, Tbilisi; [(c)] University of Georgia, Tbilisi; Georgia
[150] Department of Physics, Technion, Israel Institute of Technology, Haifa; Israel
[151] Raymond and Beverly Sackler School of Physics and Astronomy, Tel Aviv University, Tel Aviv; Israel
[152] Department of Physics, Aristotle University of Thessaloniki, Thessaloniki; Greece
[153] International Center for Elementary Particle Physics and Department of Physics, University of Tokyo, Tokyo; Japan
[154] Department of Physics, Tokyo Institute of Technology, Tokyo; Japan
[155] Department of Physics, University of Toronto, Toronto ON; Canada
[156] [(a)] TRIUMF, Vancouver BC; [(b)] Department of Physics and Astronomy, York University, Toronto ON; Canada
[157] Division of Physics and Tomonaga Center for the History of the Universe, Faculty of Pure and Applied Sciences, University of Tsukuba, Tsukuba; Japan
[158] Department of Physics and Astronomy, Tufts University, Medford MA; United States of America
[159] Department of Physics and Astronomy, University of California Irvine, Irvine CA; United States of America
[160] University of Sharjah, Sharjah; United Arab Emirates
[161] Department of Physics and Astronomy, University of Uppsala, Uppsala; Sweden
[162] Department of Physics, University of Illinois, Urbana IL; United States of America
[163] Instituto de Física Corpuscular (IFIC), Centro Mixto Universidad de Valencia - CSIC, Valencia; Spain
[164] Department of Physics, University of British Columbia, Vancouver BC; Canada
[165] Department of Physics and Astronomy, University of Victoria, Victoria BC; Canada
[166] Fakultät für Physik und Astronomie, Julius-Maximilians-Universität Würzburg, Würzburg; Germany
[167] Department of Physics, University of Warwick, Coventry; United Kingdom
[168] Waseda University, Tokyo; Japan
[169] Department of Particle Physics and Astrophysics, Weizmann Institute of Science, Rehovot; Israel
[170] Department of Physics, University of Wisconsin, Madison WI; United States of America
[171] Fakultät für Mathematik und Naturwissenschaften, Fachgruppe Physik, Bergische Universität Wuppertal, Wuppertal; Germany
[172] Department of Physics, Yale University, New Haven CT; United States of America

[a] Also Affiliated with an institute covered by a cooperation agreement with CERN.
[b] Also at An-Najah National University, Nablus; Palestine.
[c] Also at Borough of Manhattan Community College, City University of New York, New York NY; United States of America.
[d] Also at Center for High Energy Physics, Peking University; China.
[e] Also at Center for Interdisciplinary Research and Innovation (CIRI-AUTH), Thessaloniki; Greece.
[f] Also at Centro Studi e Ricerche Enrico Fermi; Italy.
[g] Also at CERN, Geneva; Switzerland.
[h] Also at Département de Physique Nucléaire et Corpusculaire, Université de Genève, Genève; Switzerland.
[i] Also at Departament de Fisica de la Universitat Autonoma de Barcelona, Barcelona; Spain.
[j] Also at Department of Financial and Management Engineering, University of the Aegean, Chios; Greece.
[k] Also at Department of Physics, Ben Gurion University of the Negev, Beer Sheva; Israel.
[l] Also at Department of Physics, California State University, Sacramento; United States of America.
[m] Also at Department of Physics, King's College London, London; United Kingdom.
[n] Also at Department of Physics, Stanford University, Stanford CA; United States of America.
[o] Also at Department of Physics, Stellenbosch University; South Africa.
[p] Also at Department of Physics, University of Fribourg, Fribourg; Switzerland.
[q] Also at Department of Physics, University of Thessaly; Greece.
[r] Also at Department of Physics, Westmont College, Santa Barbara; United States of America.
[s] Also at Hellenic Open University, Patras; Greece.
[t] Also at Institucio Catalana de Recerca i Estudis Avancats, ICREA, Barcelona; Spain.
[u] Also at Institut für Experimentalphysik, Universität Hamburg, Hamburg; Germany.
[v] Also at Institute for Nuclear Research and Nuclear Energy (INRNE) of the Bulgarian Academy of Sciences, Sofia; Bulgaria.
[w] Also at Institute of Applied Physics, Mohammed VI Polytechnic University, Ben Guerir; Morocco.
[x] Also at Institute of Particle Physics (IPP); Canada.

[y] Also at Institute of Physics and Technology, Mongolian Academy of Sciences, Ulaanbaatar; Mongolia.
[z] Also at Institute of Physics, Azerbaijan Academy of Sciences, Baku; Azerbaijan.
[aa] Also at Institute of Theoretical Physics, Ilia State University, Tbilisi; Georgia.
[ab] Also at L2IT, Université de Toulouse, CNRS/IN2P3, UPS, Toulouse; France.
[ac] Also at Lawrence Livermore National Laboratory, Livermore; United States of America.
[ad] Also at National Institute of Physics, University of the Philippines Diliman (Philippines); Philippines.
[ae] Also at Technical University of Munich, Munich; Germany.
[af] Also at The Collaborative Innovation Center of Quantum Matter (CICQM), Beijing; China.
[ag] Also at TRIUMF, Vancouver BC; Canada.
[ah] Also at Università di Napoli Parthenope, Napoli; Italy.
[ai] Also at University of Chinese Academy of Sciences (UCAS), Beijing; China.
[aj] Also at University of Colorado Boulder, Department of Physics, Colorado; United States of America.
[ak] Also at Washington College, Chestertown, MD; United States of America.
[al] Also at Yeditepe University, Physics Department, Istanbul; Türkiye.
[*] Deceased.